Full-Potential, Euler, and Navier-Stokes Schemes

Antony Jameson*
Princeton University, Princeton, New Jersey

Introduction

THE purpose of this chapter is to survey some of the highlights of computational fluid dynamics (CFD) schemes for solving the full-potential, Euler, and Navier-Stokes equations. Prior to the advent of the computer, there was a rather comprehensive mathematical formulation of fluid mechanics already in place. This formulation had been developed by elegant mathematical analysis, frequently guided by brilliant insights. Well-known examples include the airfoil theory of Kutta and Joukowski, Prandtl's wing and boundary-layer theories, von Kármán's analysis of the vortex street, and, more recently, Jones' slender wing theory[1] and Hayes' theory of linearized supersonic flow.[2] These methods require simplifying assumptions of various kinds and cannot be used to make quantitative predictions of complex flows dominated by nonlinear effects. The computer opens up new possibilities for attacking these problems by direct calculation of solutions to more complete mathematical models.

The main uses of CFD in aeronautical science fall into two broad categories. First, there is the objective of providing reliable aerodynamic predictions, which will enable designers to produce better airplanes. Second, there is the possibility of using CFD for purely scientific investigations. It seems possible that numerical simulation of complex flows not readily accessible to experimental measurements can provide new insights into the underlying physical processes. In particular, computational methods offer a new tool for the study of structures in turbulent flow and the mechanisms of transition from laminar to turbulent flow.

Most of this chapter is devoted to the use of computational methods for aerodynamic prediction. This is a comparatively recent development. Prior to 1965 computational methods were hardly used in aerodynamic analysis, although they were already widely used for structural analysis. The primary tool for the development of aerodynamic configurations was the wind tunnel. Experimental aerodynamicists could arrive at efficient shapes

*James S. McDonnell Professor, Department of Aerospace Engineering.

through testing guided by good physical insight. Notable examples of the power of this method include Whitcomb's discovery of the area rule for transonic flow and his subsequent development of aft-loaded supercritical airfoils.[3,4] By the 1960s it began to be recognized that computers had become powerful enough to make it worthwhile to attempt calculations of aerodynamic properties of at least isolated components of an aircraft. It was also apparent that, depending on the intended application, useful simulations might be achieved with a range of mathematical models of varying complexity. Commercial aircraft fly largely with attached flows, in which the viscous effects are confined to the boundary layer. Consequently, they have a relatively small effect on the global flow pattern, other than their role in establishing circulatory flows through the shedding of start-up vortices off the trailing edges of lifting surfaces. Inviscid flow predictions then serve a useful role and can take advantage of irrotationality to simplify the equations through the introduction of a velocity potential. This reduction led to the first major advance, the introduction of panel methods to solve the linearized potential-flow equation. The initial demonstration of this approach by Hess and Smith[5] was soon followed by its extension to lifting flows[6] and to linearized supersonic flow.[7]

The 1970s saw widespread efforts to develop methods of predicting transonic flows with shock waves, which required the use of a nonlinear mathematical model. The first major breakthrough was the scheme of Murman and Cole[8,9] for treating the transonic small-disturbance equation. This was the catalyst for widespread development of methods for calculating transonic potential flows in two and three dimensions using either the small-disturbance equation or the full-potential-flow equation.

In parallel, efforts were underway to devise efficient algorithms for solving the Euler and Navier-Stokes equations. Following the pioneering efforts of Magnus and Yoshihara,[10] MacCormack introduced his famous explicit difference scheme in 1970.[11] Efforts to improve efficiency led to the implicit scheme of Beam and Warming,[12] which was extended to general curvilinear coordinates by Steger.[13] The need to find a better shock-capturing method was also apparent and stimulated the introduction of flux splitting.[14] By 1979, however, Euler methods remained very expensive and had not attained levels of accuracy that justified their routine use for engineering design. The GAMM Workshop of 1979 served to highlight the deficiencies of the methods then available.[15] Nevertheless, it was already evident that advances in the available computing power would soon make it entirely feasible to solve the three-dimensional Euler equations, and the 1980s have seen widespread efforts to realize this objective. The alternating-direction method has been systematically developed into an effective tool, and the current state of the art is represented by ARC2D and ARC3D.[16] Implicit schemes using LU decomposition[17] and relaxation have also proved successful. A parallel path of development that has also led to efficient programs has been the use of multistage explicit time-stepping schemes.[18] The author's FLO52 and FLO57 programs using this concept have been widely used. Stemming from the mathematical theory of shock waves, procedures have also been developed for the design of effective shock-capturing schemes. There have been intensive efforts to find more

rapidly convergent methods to find steady-state solutions. In particular, the use of multiple grids, first introduced by Fedorenko[19] and subsequently developed by Brandt,[20] has been extended to the treatment of hyperbolic systems[21-23] and has proved to be extremely effective.

We are now at a point where a variety of efficient algorithms for the solution of the Euler and Navier-Stokes equations have been developed, and the principles underlying their construction are quite well understood. Their application to date has largely been limited to relatively simple configurations because of the difficulty of generating meshes around complex shapes. Viscous effects in attached flows can be fairly well predicted by making boundary-layer corrections. Military aircraft frequently fly in conditions of separated flow. The appropriate mathematical model is then the Navier-Stokes equations. At Reynolds numbers typical of full-scale flight, however, the flow becomes turbulent, and the disparity of scales in a turbulent flow is so large that direct simulation is probably not feasible without radical developments in computer technology. Therefore, it becomes necessary to resort to Reynolds averaging, and the equations must be closed by a turbulence model. Progress in simulating separated viscous flows may now be more dependent on improvement in turbulence modeling than it is on algorithm development.

Computational aerodynamics has reached a point of maturity where it may be worthwhile to take stock of the present situation and to consider which directions of future efforts are likely to be most profitable. In this chapter some of the algorithmic concepts believed to be a foundation for future developments will be identified. It seems useful for this purpose first to consider the objectives of computational aerodynamics. Three levels of desirable performance can be identified:

1) the capability of predicting the flow past airplanes in different flight regimes (takeoff, cruise at transonic speed, flutter);

2) the interactive calculations to allow immediate improvement of the design; and

3) the integration of the predictive capability into an automatic design method using computer optimization and artificial intelligence.

To date not even the first level has been fully realized for all regimes of flight. Some methods are fast enough that the second level is already feasible, say, for airfoil evaluation. Some pioneering attempts have been made at the third level, and it is clear that advances in computational power and algorithmic efficiency will make this feasible for useful applications within the coming decade.

It is also important to understand what kind of information the designer may be seeking. For the final design he may need accurate quantitative predictions of design parameters such as the lift and drag coefficients. In the early stages he may be more interested in acquiring a qualitative understanding of the nature of the flowfield and the impact of design changes on the onset of separation, for example, or the location of the regions of separated flow.

The requirements to be met by an effective method include the following:

1) the capability of simulating the main features of the flow, such as shock waves and vortex sheets;

2) the prediction of viscous effects;
3) the ability to handle geometrically complex configurations; and
4) the efficiency in both computational and human effort.

In any case it is clear that the value of the information provided must be measured against the cost of producing it. In the application of computer simulations to engineering design, we can therefore anticipate that simplified mathematical models will continue to be useful for preliminary estimations and tradeoff studies for which full details of the flowfield are not essential. On the other hand, there is a pervasive need to predict flows over exceedingly complex configurations, and future computational methods must be designed to address this requirement.

The remaining sections review some of the main algorithmic developments of the past two decades in this context. The next section reviews the mathematical models. The section on algorithms for potential flow covers potential-flow methods and the section on algorithms for Euler equations and the section on viscous flow calculations cover methods for the full inviscid and viscous equations. In the conclusion, I try to identify what I believe to be the principal remaining problems, including algorithmic issues such as the construction of schemes with a higher order of accuracy, convergence acceleration, and shock-capturing or front-tracking schemes, and also computer science issues such as concurrent calculation on vector, pipelined, or parallel processors; optimization and design techniques; and expert systems.

Mathematical Models of Fluid Flow

The equations for flow of a gas in thermodynamic equilibrium are the Navier-Stokes equations. Let ρ, u, v, E, and p be the density, Cartesian velocity components, total energy, and pressure, respectively, and let x and y be Cartesian coordinates. Then, for a two-dimensional flow these equations can be written as

$$\frac{\partial \boldsymbol{w}}{\partial t}+\frac{\partial \boldsymbol{f}}{\partial x}+\frac{\partial \boldsymbol{g}}{\partial y}=\frac{\partial \boldsymbol{R}}{\partial x}+\frac{\partial \boldsymbol{S}}{\partial y} \tag{1}$$

where $\boldsymbol{w}$ is the vector of dependent variables, and $\boldsymbol{f}$ and $\boldsymbol{g}$ are the convective flux vectors:

$$\boldsymbol{w}=\begin{bmatrix}\rho\\ \rho u\\ \rho\\ \rho E\end{bmatrix},\quad \boldsymbol{f}=\begin{bmatrix}\rho u\\ \rho u^2+p\\ \rho uv\\ \rho uH\end{bmatrix},\quad \boldsymbol{g}=\begin{bmatrix}\rho v\\ \rho vu\\ \rho v^2+p\\ \rho vH\end{bmatrix} \tag{2}$$

Here H is the enthalpy,

$$H=E+\frac{p}{\rho}$$

and the pressure is obtained from the equation of state

$$p = (\gamma - 1)\rho[E - \tfrac{1}{2}(u^2 + v^2)] \tag{3}$$

The flux vectors for the viscous terms are

$$\boldsymbol{R} = \begin{bmatrix} 0 \\ \tau_{xx} \\ \tau_{xy} \\ u\tau_{xx} + v\tau_{xy} \end{bmatrix}, \qquad \boldsymbol{S} = \begin{bmatrix} 0 \\ \tau_{xy} \\ \tau_{yy} \\ u\tau_{xy} + v\tau_{yy} \end{bmatrix} \tag{4}$$

where the viscous stresses are

$$\tau_{xx} = 2\mu u_x - \frac{2\mu}{3}(u_x + v_y)$$

$$\tau_{yy} = 2\mu v_y - \frac{2\mu}{3}(u_x + v_y)$$

$$\tau_{xy} = \mu(u_y + v_x)$$

and μ is the coefficient of viscosity. The computational requirements for the simulation of turbulent flow have been estimated by Chapman.[24] They are clearly beyond the reach of current computers.

The first level of approximation is to resort to time averaging of rapidly fluctuating components. This yields the Reynolds equations, which require a turbulence model for closure. Since a universally satisfactory turbulence model has yet to be found, current turbulence models have to be tailored to the particular flow. The Reynolds equations can be solved with computers of the class of the Cray 1 or Cyber 205, at least for two-dimensional flows, such as flows over airfoils.

The next level of approximation is to eliminate viscosity. Equation (1) then reduces to the Euler equation

$$\frac{\partial \boldsymbol{w}}{\partial t} + \frac{\partial \boldsymbol{f}}{\partial x} + \frac{\partial \boldsymbol{g}}{\partial y} = 0 \tag{5}$$

It is quite feasible to solve complex three-dimensional flows with this model, as will be discussed.

If we assume the flow to be irrotational, we can introduce a velocity potential ϕ and set

$$u = \phi_x, \qquad v = \phi_y$$

The Euler equation [Eq. (5)] now reduces to the potential-flow equation

$$\frac{\partial}{\partial x}(\rho\phi_x) + \frac{\partial}{\partial y}(\rho\phi_x) = 0 \tag{6}$$

or, in quasilinear form,

$$(c^2 - u^2)\phi_{xx} - 2uv\phi_{xy} + (c^2 - v^2)\phi_{yy} = 0 \tag{7}$$

where c is the speed of sound. This is given by

$$c^2 = \frac{\gamma p}{\rho}$$

where γ is the ratio of specific heats. According to Crocco's theorem, vorticity in a steady flow is associated with entropy production through the relation

$$q \times \zeta + T \cdot \nabla S = 0$$

where q and ζ are the velocity and vorticity vectors, respectively, T is the temperature, and S is the entropy. Thus, the introduction of a potential is consistent with the assumption of isentropic flow. Then, if M_∞ is the freestream Mach number, the units may be normalized so that

$$p = \frac{\rho^\gamma}{\gamma M_\infty^2}, \qquad \rho = (M_\infty^2 c^2)^{1/\gamma - 1} \tag{8}$$

while the local speed of sound can be determined from the energy equation, written as

$$\frac{c^2}{\gamma - 1} + \frac{q^2}{2} = \frac{1}{(\gamma - 1)M_\infty^2} + \frac{1}{2} \tag{9}$$

Because shock waves generate entropy, they cannot be exactly modeled by the potential-flow equation. However, weak solutions admitting isentropic jumps that conserve mass but not momentum are a good approximation to shock waves, as long as the shock waves are quite weak (with a Mach number < 1.3 for the normal velocity component upstream of the shockwave). Stronger shock waves tend to separate the flow, with the result that the inviscid approximation is no longer adequate. Thus, this model is well balanced and has proved extremely useful for estimating the cruising performance of transport aircraft.

If one assumes small disturbances and a Mach number close to unity, the potential equation can be reduced to the transonic small-disturbance equation. A typical form is

$$[1 - M_\infty^2 - (\gamma + 1)M_\infty^2 \phi_x]\phi_{xx} + \phi_{yy} = 0 \tag{10}$$

Finally, if the freestream Mach number is not close to unity, the potential-flow equation can be linearized as

$$(1 - M_\infty^2)\phi_{xx} + \phi_{yy} = 0 \tag{11}$$

Algorithms for Potential Flow

Overview

Although the Euler- and Reynolds-averaged Navier-Stokes equations can now be solved with quite moderate computational costs, algorithms for potential flow remain useful because they can provide extremely inexpensive quick estimates. Also, certain ideas for shock-capturing and convergence acceleration that were first developed for potential-flow calculations have proved transferable to more complex models such as the Euler equations.

Upwind Differencing

When the potential-flow equation [Eq. (6)] is used to predict transonic flows, the difficulty arises that the solution is invariant under a reversal of the velocity vector ($u = -\phi_x, v = -\phi_y$). Consider a transonic flow past an ellipse with a compression shock wave. Then there is a corresponding solution with an expansion shock wave (see Figs. 1a and 1b). In fact, a central-difference scheme would preserve fore-and-aft symmetry, leading to a solution of the type illustrated in Fig. 1c. In 1970 the landmark paper of Murman and Cole[8] appeared. This demonstrated a simple way to obtain physically relevant solutions of the transonic small-disturbance equation [Eq. (10)]. Writing this equation as

$$A\phi_{xx} + \phi_{yy} = 0 \tag{12}$$

where A is the nonlinear coefficient in Eq. (10), they proposed the use of central differencing if $A > 0$ (subsonic flow), but upwind differencing for ϕ_{xx} if $A < 0$ (supersonic flow), as illustrated in Fig. 2. The equations were then solved by a line-relaxation scheme, in which the unknowns were determined simultaneously on each successive vertical line, marching in the streamwise direction. The scheme amounted to a combination of a relaxation method for the subsonic zone, in which the equation is elliptic, with an implicit scheme for the wave equation in the supersonic zone.

This work was extremely important both because it pointed the way to reasonably inexpensive simulations of transonic flows and also because it demonstrated for the first time the possibility of an effective shock-capturing scheme with a sharp, nonoscillatory discrete shock structure. Within the next few years the concept of Murman and Cole was generalized to the full transonic potential-flow equation and applied to a wide variety of flow simulations.

In order to treat the full quasilinear potential-flow equation [Eq. (7)], one may rewrite it in a coordinate system locally aligned with the flow. Equation (7) then becomes

$$(c^2 - q^2)\phi_{ss} + c^2\phi_{nn} = 0$$

where

$$\phi_{ss} = \frac{u^2}{q^2}\phi_{xx} + \frac{2uv}{q^2}\phi_{xy} + \frac{v^2}{q^2}\phi_{yy}$$

and

$$\phi_{nn} = \frac{v^2}{q^2}\phi_{xx} - \frac{2uv}{q^2}\phi_{xy} + \frac{u^2}{q^2}\phi_{yy}$$

Upwind differencing is now used for all second derivatives contributing to ϕ_{ss} whenever $q > c$. This leads to Jameson's rotated difference scheme[25] (see also Albone[26]). A convergent iterative scheme can be derived by regarding the iterations as time steps in an artificial time coordinate. The principal part of the equivalent time-dependent equation has the form

$$(M^2 - 1)\phi_{ss} - \phi_{nn} + 2\alpha\phi_{st} + 2\beta\phi_{nt} = 0$$

Introducing a new time coordinate

$$T = t - \frac{\alpha s}{M^2 - 1} + \beta n$$

this becomes

$$(M^2 - 1)\phi_{ss} - \phi_{nn} - \left(\frac{\alpha^2}{M^2 - 1} - \beta^2\right)\phi_{TT} = 0$$

If the flow is locally supersonic, T is spacelike and either s or n is timelike. Since s is the timelike direction in the steady-state problem, and the time-dependent problem is compatible with the steady-state problem only if

$$\alpha^2 > \beta^2(M^2 - 1)$$

This generally requires the explicit addition of a term in ϕ_{st}.

In his paper of 1973, Murman recognized that the switch in the difference scheme could violate the conservative form of the equations, leading to shock jumps that violated the conservation of mass.[9] This difficulty can be corrected by reformulating the switch to upwind differencing by the introduction of artificial viscosity. The dominant discretization error in the upwind difference formula for ϕ_{xx} is $-\Delta x\phi_{xxx}$, and terms of this nature can be added explicity in conservation form, leading to special transition operators across the sonic line. An appropriate form of artificial viscosity for the potential flow equation [Eq. (6)] is a difference approximation to

$$\Delta x \frac{\partial}{\partial x}\mu|u|\rho_x + \Delta y \frac{\partial}{\partial y}\mu|v|\rho_y$$

where Δx and Δy are the mesh widths, and μ is a switch function

$$\mu = \max\left\{0, 1 - \frac{1}{M^2}\right\}$$

which cuts off the viscosity in the subsonic zone.[27] It was realized by several authors that a term of this kind can be added simply by biasing the density in an upwind direction.[28-30] This has facilitated the development of discretizations on arbitrary subdivisions of the domain into hexahedrons or tetrahedrons.

Convergence Acceleration

Transonic flow calculations by relaxation methods generally require a very large number of iterations to converge (on the order of 500–2000). This inhibited the more widespread use of these methods, particularly for three-dimensional calculations, and stimulated numerous efforts to find more rapidly convergent methods. The two most effective approaches have been approximate factorization of the difference operator and acceleration by the use of multiple grids.

Let the difference equations be written as

$$L\phi = 0 \tag{13}$$

where L is a nonlinear difference operator, and ϕ is the solution vector. Then a typical iterative scheme can be written as

$$N\delta\phi + L\phi^n = 0 \tag{14}$$

where $\delta\phi$ is the correction, and N is a linear operator that can be inverted relatively cheaply and should approximate L (in the linear case the error is reduced at each cycle by $I - N^{-1}L$). In an approximate factorization method, N is formed as a product

$$N = N_1 N_2 \ldots N_q$$

of easily invertible operators. Ballhaus et al.[31] found that a good choice for the small-disturbance equation [Eq. (12)] is

$$(\alpha - AD_x^{\sim})(\alpha D_x^- - D_y^+)\delta\phi + \alpha L\phi^-$$

where D_x^+ and D_x^- are forward- and backward-difference operators, and

$$D_x^{\sim} = \begin{cases} D_x^+ & \text{if} \quad A > 0 \\ D_x^- & \text{if} \quad A < 0 \end{cases}$$

Very efficient schemes of this type have been developed for the transonic potential-flow equation by Holst.[32]

The multigrid method was first proposed by Fedorenko,[19] and some promising results for the small-disturbance equation were obtained by Brandt and South.[33] The idea is to use corrections calculated on a sequence of successively coarser grids to improve the solution on a fine grid. Consider a linear problem and let

$$L_h \phi_h = 0 \tag{15}$$

be the discrete equations for a mesh with a spacing proportional to h. Let u_h be an estimate of ϕ_h, and let v_h be a correction that should reduce $L_h(u_h + v_h)$ to zero. Then, instead, one can write an equation for v on a mesh with twice as large a spacing:

$$L_{2h} v_{2h} + Q_{2h}^h L_h u_h = 0 \tag{16}$$

where Q_{2h} is a collection operator that forms a weighted average of the residuals on the fine grid in the neighborhood of each mesh point of the coarse grid. The correction is finally interpolated back to the fine grid:

$$u_h^{\text{new}} = u_h + P_h^{2h} v_{2h} \tag{17}$$

where P_h^{2h} is an interpolation operator. Corrections to the solution of Eq. (16) can in turn be calculated on a still coarser grid, and so on. The same basic iterative scheme can be used on all of the grids in the sequence. It has been proved that solutions to elliptic problems with N unknowns can be obtained in $\mathcal{O}(N)$ operations by the use of multiple grids.[34] A condition for the successful use of multiple grids is that, before passing to a coarser grid, the high-frequency error modes should be reduced to the point that the remaining error can be properly resolved on the coarser grid.

The method can be reformulated for a nonlinear problem by explicitly introducing the solution vector u_{2h} on the coarse grid. An updated solution vector $\bar{u}_{2h}$ is then calculated from the equation

$$L_{2h} \bar{u}_{2h} + Q_{2h}^h L_h u_h - L_{2h} u_h = 0$$

where the difference between the collected residuals from neighboring points on the fine grid and the residual calculated on the coarse grid appears as a forcing function. The correction $\bar{u}_{2h} - u_{2h}$ is then interpolated back to the fine grid.

Figure 3 shows the result of a calculation in which a generalized alternating-direction (ADI) method was used to drive the multigrid iteration.[35] The ADI scheme differs from the standard ADI scheme in replacing the scalar parameter by a difference operator (which also operates on the residuals). The purpose of this is to retain a well-posed problem in the supersonic zone. An efficient strategy is to use a simple V cycle in which one ADI iteration is performed on each grid until the coarsest grid is reached, and then one ADI iteration on each grid on the way back up to the fine grid. A solution on a 192×32 grid accurate to four figures was

obtained by 3 V cycles on a 48×8 grid, followed by three V cycles on a 96×16 grid, and 3 V cycles on the 192×32 grid. The total calculation is equivalent to 4 V cycles on the 192×32 grid. It seems likely that this must be close to the lower bound for the number of operations required to solve 6144 simultaneous nonlinear equations.

Treatment of Complex Geometry

An effective approach to the treatment of two-dimensional flows over complex profiles is to map the exterior domain conformally onto the unit disk.[25] Equation (6) is then written in polar coordinates as

$$\frac{\partial}{\partial \theta}\left(\frac{\rho}{r}\phi_\theta\right) + \frac{\partial}{\partial r}(r\rho\phi_r) = 0$$

where the modulus h of the mapping function enters only in the calculation of the density from the velocity

$$q = \frac{\nabla\phi}{h}$$

This procedure is very accurate.

Applications to complex three-dimensional configurations require a more flexible method of discretization, such as that provided by the finite-element method. Jameson and Caughey[36] proposed a scheme using isoparametric bilinear or trilinear elements. The discrete equations can most conveniently be derived from the Bateman variational principle. This states that the integral

$$I = \int\int p \, dx \, dy$$

is stationary in two-dimensional potential flow. It follows from Eqs. (8) and (9) that

$$\frac{\partial p}{\partial u} = -\rho u, \qquad \frac{\partial p}{\partial v} = -\rho v$$

whence, in potential flow,

$$\delta I = -\int\int (\rho u \delta\phi_x + \rho v \delta\phi_y) \, dx \, dy$$

and Eq. (6) is recovered on integrating by parts and allowing arbitrary variation $\delta\phi$. In the scheme of Jameson and Caughey I is approximated as

$$I = \Sigma P_k V_k$$

where p_k is the pressure at the center of the kth cell, and V_k is its area (or volume), and the discrete equations are obtained by setting the derivative of I with respect to the nodal values of potential to zero. Artificial viscosity is added to give an upwind bias in the supersonic zone, and an iterative scheme is derived by embedding the steady-state equation in an artificial, time-dependent equation. Several widely used codes (FLO27, FLO28, FLO30) have been developed using this scheme.

An alternative approach to the treatment of complex configurations has been developed by Bristeau et al.[37] Their method uses a least-squares formulation of the problem, together with an iterative scheme derived with the aid of optimal control theory. The method could be used in conjunction with a subdivision into either quadrilaterals or triangles, but in practice triangulations have been used. The least-squares method in its basic form allows expansion shocks. In early formulations these were eliminated by penalty functions. It was subsequently found to be best to use upwind biasing of the density. The method has been extended at Avions Marcel Dassault to the treatment of extremely complex three-dimensional configurations, using a subdivision of the domain into tetrahedrons. A striking success was achieved in 1982 with the first simulation of transonic flow past a complete aircraft by solution of the full quasilinear potential-flow equation, as illustrated in Fig. 4.

Algorithms for the Euler Equations

Overview: Time-Dependent Formulation

In parallel with the development of effective algorithms for potential flow, there were ongoing efforts to derive fast, accurate, and reliable methods for solving the Euler equations. Steady-state solutions are typically needed for design applications. The introduction of a space discretization procedure then reduces the problem to the solution of a large number of coupled nonlinear equations. These equations might be solved by a variety of iterative methods. Two possibilities in particular are the least-squares method[37] and the Newton iteration.[38] However, it has generally been found expedient to use the time-dependent equations as a vehicle for reaching the steady state. Some advantages of this strategy include the following:

1) The strategy is simple.

2) It is possible to use the same computer program to calculate steady and unsteady flows.

3) The time-dependent problem provides a natural framework for the design of nonoscillatory shock-capturing schemes that reflect the physics of wave propagation.

4) Algorithms can be devised for concurrent computation on vector, pipelined, or parallel processors either through the use of an explicit time-stepping scheme or through the use of an iterative procedure at each time step of an implicit scheme.

It has also been found that satisfactory schemes should be designed to conform to some general guidelines. Some of these include the following:

1) The conservation laws of gasdynamics should be satisfied in discrete form by the numerical approximation.

2) Shock waves and contact discontinuities should be automatically captured by the difference scheme.

3) In steady flow calculations the final steady state should be independent of the time-stepping scheme.

4) Invariant quantities in the flowfield, such as entropy upstream of a shock wave or total enthalpy in a steady flow, should also be invariant in the numerical solution.

5) Uniform flow should be an exact solution of the difference equations on an arbitrary mesh.

An alternative to guideline 2 is automatic detection of shock waves in conjunction with front tracking. In this case guideline 1, which is needed to ensure the satisfaction of correct jump conditions by a shock-capturing scheme,[39] is no longer strictly necesssary, but it remains desirable since it ensures global conservation of mass, momentum, and energy.

The early standard for time-stepping methods was set by the two-stage scheme of MacCormack,[11] which has been very widely used. To solve the one-dimensional system

$$\frac{\partial w}{\partial f} + \frac{\partial}{\partial x} f(w) = 0 \tag{18}$$

the scheme advances from time level n to time level $n+1$ by setting

$$\tilde{w} = w^n - \Delta t D_x^+ f(w^n)$$

and

$$w^{n+1} = w^n - \frac{\Delta t}{2} D_x^+ [f(w^n) + D_x^- f(\tilde{w})] \tag{19}$$

where the superscripts denote the time level, and D_x^+ and D_x^- are forward- and backward-difference operators approximating $\partial/\partial x$:

$$D_x^+ f_i = \frac{f_{i+1} - f_i}{\Delta x}, \qquad D_x^- f_i = \frac{f_i - f_{i-1}}{\Delta y}$$

The value at the end of the time step is first predicted using forward differences, and then the predicted value is used in the calculation of the final corrected value w^{n+1} by a formula that is centered about the middle of the time step.

This is the simplest known two-level scheme that is both stable and second-order-accurate. Additional dissipative terms have to be introduced to eliminate oscillations in the vicinity of shock waves. The scheme also does not satisfy principle 3, since it yields a steady state that depends on the

time step Δt. Nor is the enthalpy constant in discrete steady solutions. However, the algorithm performs well in the absence of discontinuities in the flow.

A convenient way to meet requirement 3 is to separate the space-marching procedure entirely from the time-marching procedure by applying first a semidiscretization. This has the advantage of allowing the problems of spatial discretization error, artificial dissipation, and shock modeling to be studied independently of the problems of time-marching stability and convergence acceleration.

Space Discretization of the Euler Equations

Following the lead of MacCormack and Paullay,[40] the space discretization of the Euler equation [Eq. (5)] can be derived in a very natural way from the integral form

$$\frac{\partial}{\partial t}\int_S w\, dS + \int_{\partial S} [f(w)\, dy - g(w)\, dx] = 0 \tag{20}$$

for a domain S with boundary ∂S.

If we divide the domain into a large number of small subdomains, we can use Eq. (20) to estimate the average rate of change of w in each subdomain. This is an effective method to obtain discrete approximations to Eq. (5), which preserve its conservation form. In general, the subdomains could be arbitrary, but it is convenient to use either quadrilateral or triangular cells. Correspondingly, it is convenient to use either distorted cubic or tetrahedral cells in three-dimensional calculations. Alternative discretizations may be obtained by storing sample values of the flow variables at either the cell centers or the cell corners. These variations are illustrated in Fig. 5 for a two-dimensional case.

Figures 5a and 5b show cell-centered schemes on rectilinear and triangular meshes.[18,41] In either case Eq. (20) is written for the cell labeled 0 as

$$\frac{d}{dt}(Sw) + Q = 0 \tag{21}$$

where S is the cell area, and Q is the net flux out of the cell. This can be approximated as

$$Q = \sum_k (\bar{f}_{0k}\, \Delta y_{0k} - \bar{g}_{0k}\, \Delta x_{0k}) \tag{22}$$

where the sum is over the edges of cell 0, Δx_{0k} and Δy_{0k} are measured along the edge separating cell 0 from cell k, and the flux vectors $\bar{f}_{0k}$ and $\bar{g}_{0k}$ are evaluated by taking the average of their values in cell 0 and cell k:

$$\bar{f}_{0k} = \tfrac{1}{2}(f_0 + f_k), \qquad \bar{g}_{0k} = \tfrac{1}{2}(g_0 + g_k) \tag{23}$$

An alternative averaging procedure is to multiply the average value of the convected quantity, ρ_{0k}, in the case of the continuity equation, for example, by the rate of transport

$$Q_{0k} = \tfrac{1}{2}(u_0 + u_k)\,\Delta y_{0k} - \tfrac{1}{2}(v_0 + v_k)\,\Delta x_{0k} \tag{24}$$

obtained by taking the inner product of the mean of the velocity vector $\boldsymbol{q}$ with the unit normal multiplied by the edge length.

Figures 5c and 5d show corresponding schemes on rectilinear and triangular meshes in which the flow variables are stored at the vertices.[42] We can now form a control volume for each vertex by taking the union of the cells meeting at that vertex. Equation (21) then takes the form

$$\frac{\mathrm{d}}{\mathrm{d}t}\left(\sum_k V_k\right)w + \sum_k Q_k = 0 \tag{25}$$

where V_k and Q_k are the area and flux balance, respectively, for the kth cell in the control volume. The flux balance for a given cell is now approximated as

$$Q = \sum_\ell (\bar{f}_\ell\,\Delta y_\ell - \bar{f}_\ell\,\Delta x_\ell) \tag{26}$$

where Δx_ℓ and Δy_ℓ are measured along the ℓth edge, and f_ℓ and g_ℓ are estimates of the mean flux vectors across that edge. Fluxes across internal edges cancel when the sum $\Sigma_k Q_k$ is taken in Eq. (25), so that only the external edges of the control volume contribute to its flux balance. The mean flux vector across an edge can be conveniently approximated as the average of the values at its two endpoints,

$$\bar{f}_{12} = \tfrac{1}{2}(f_1 + f_2), \qquad \bar{g}_{12} = \tfrac{1}{2}(g_1 + g_2)$$

in Fig. 5c or 5d, for example. The sum $\Sigma\, Q_k$ in Eq. (25), which then amounts to a trapezoidal integration rule around the boundary of the control area, should remain fairly accurate even when the mesh is irregular.

Dissipation, Upwinding, and Total Variation Diminishing Schemes

Equations (21) and (22) represent nondissipative approximations to the Euler equations. Dissipative terms may be needed for two reasons. First, there is the possibility of undamped oscillatory modes. For example, when either a cell-centered or a vertex formulation is used to represent a conservation law on a rectilinear mesh, a mode with values ± 1 alternately at odd and even points leads to a numerically evaluated flux balance of zero in every interior control volume. Although the boundary conditions may suppress such a mode in the steady-state solution, the absence of damping at interior points may have an adverse effect on the rate of convergence to the steady state.

The second reason for introducing dissipative terms is to allow the clean capture of shock waves and contact discontinuities without undesirable oscillations. Following the pioneering work of Godunov,[43] a variety of dissipative and upwind schemes designed to have good shock-capturing properties have been developed during the past decade.[44-53] The one-dimensional scalar conservation law

$$\frac{\partial u}{\Delta t} + \frac{\partial}{\partial x} f(u) = 0 \tag{27}$$

provides a useful model for the analysis of these schemes. The total variation

$$\mathrm{TV} = \int_{-\infty}^{\infty} \left| \frac{\partial u}{\partial x} \right| dx$$

of a solution of Eq. (27) does not increase, provided that any discontinuity appearing in the solution satisfies an entropy condition.[55] The concept of total variation diminishing (TVD) difference schemes, introduced by Harten,[49] provides a unifying framework for the study of shock-capturing methods. These are schemes with the property that the total variation of the discrete solution

$$\mathrm{TV} = \sum_{-\infty}^{\infty} \left| v_j - v_{j-1} \right|$$

cannot increase. The general conditions for a multipoint one-dimensional scheme to be TVD have been stated and proved by Jameson and Lax.[56]

TVD schemes preserve the monotonicity of an initially monotone profile, because the total variation would increase if the profile ceased to be monotone. Consequently, they prevent the formation of spurious oscillations. In this simple form, however, they are at best first-order-accurate. Harten devised a second-order-accurate TVD scheme by introducing anti-diffusive terms, and flux limiters to improve shock resolution can be traced to the work of Boris and Book.[44] The concept of the flux limiting was independently advanced by Van Leer.[45] A particularly simple way to introduce a second-order-accurate TVD scheme is to introduce flux limiters directly into a higher-order dissipative term.[53]

There are difficulties in extending these ideas to systems of equations and also to equations in more than one space dimension. First, the total variation of the solution of a system of hyperbolic equations may increase. Second, it has been shown by Goodman and Leveque that a TVD scheme in two space dimensions is no better than first-order-accurate.[57]

If one wishes to use one-sided differencing, one must allow for the fact that the general one-dimensional system defined by Eq. (18) produces signals traveling in both directions. One way of generalizing one-sided differencing to a system of equations is the flux-vector-splitting method proposed by Steger and Warming.[14]

Another approach to the discretization of hyperbolic systems was originally proposed by Godunov.[43] Suppose that Eq. (18) is approximated by

$$w_i^{n+1} = w_i^n - \frac{\Delta t}{\Delta x}(F_{i+1/2} - F_{i-1/2}) \tag{28}$$

where the numerical flux function $F_{i+1/2} = F(w_i, w_{i+1})$ is an approximation to the flux across the cell boundary $x_{i+1/2}$. This function must satisfy the consistency condition $F(w, w) = F(w)$. In the Godunov scheme $F_{i+\frac{1}{2}}$ is taken to be the flux value arising at $x_{i+1/2}$ in the exact solution of the initial value problem defined by piecewise constant data between each cell boundary. This simulates the motion of both shocks and expansion fans, but it is expensive.

Various simpler schemes designed to distinguish between the influence of forward- and backward-moving waves have recently been developed, based on the concept of flux difference splitting introduced by Roe.[47]

The use of flux splitting allows precise matching of the dissipative terms to introduce the minimum amount of dissipation needed to prevent oscillations. This in turn reduces the thickness of the numerical shock layer to the minimum attainable, one or two cells for a normal shock. In practice, however, it turns out that shock waves can be quite cleanly captured without flux splitting by using adaptive coefficients. The dissipation then has a low background level that is increased in the neighborhood of shock waves to a peak value proportional to the maximum local wave speed. The second difference of the pressure has been found to be an effective measure for this purpose. The dissipative terms are constructed in a similar manner for each dependent variable by introducing dissipative fluxes that preserve the conservation form.

For a two-dimensional rectilinear mesh the added terms have the form

$$d_{i+\frac{1}{2},j} - d_{i-\frac{1}{2},j} + d_{i,j+\frac{1}{2}} - d_{i,j-\frac{1}{2}} \tag{29}$$

These fluxes are constructed by blending first and third differences of the dependent variables. For example, the dissipative flux in the i direction for the mass equation is

$$d_{i+\frac{1}{2},j} = R(\epsilon^{(2)} - \epsilon^{(4)}\delta_x^2)(\rho_{i+1,j} - \rho_{i,j}) \tag{30}$$

where δ_x^2 is the second difference operator, $\epsilon^{(2)}$ and $\epsilon^{(4)}$ are the adaptive coefficients, and R is a scaling factor proportional to an estimate of the maximum local wave speed normal to the cell boundary. The coefficient $\epsilon^{(4)}$ provides the background dissipation in smooth parts of the flow and can be used to improve the capability of the scheme to damp high-frequency modes. Shock capturing is controlled by the coefficient $\epsilon^{(2)}$, which is made proportional to the normalized second difference of the pressure

$$v_{i,j} = \left|\frac{p_{i+1,j} - 2p_{i,j} + p_{i-1,j}}{p_{i+1,j} + 2p_{i,j} + p_{i-1,j}}\right|$$

in the adjacent cells.

Schemes constructed along these lines combine the advantages of simplicity and economy of computation, at the expense of an increase in thickness of the numerical shock layer to three or four cells. They have also proved robust in calculations over a wide range of Mach numbers (extending up to 20 in recent studies[58]). They can also be quite easily modified for calculations on triangular or tetrahedral meshes.[42]

Time-Stepping Schemes

The discretization procedures of the section on mathematical models of fluid flow lead to a set of coupled ordinary differential equations, which can be written in the form

$$\frac{dw}{dt} + R(w) = 0 \tag{31}$$

where w is the vector of the flow variables at the mesh points, and $R(w)$ is the vector of the residuals, consisting of the flux balances defined by Eqs. (21) or (25), together with the added dissipative terms. These are to be integrated to a steady state. Since the objective is simply to reach the steady state, and details of the transient solution are immaterial, the time-stepping scheme may be designed solely to maximize the rate of convergence without having to meet any constraints imposed by the need to achieve a specified level of accuracy, provided that it does not interfere with the definition of the residual $R(w)$. Figure 6 indicates some of the principal time-stepping schemes that might be considered. The first major choice is whether to use an explicit or an implicit scheme.

Explicit schemes that might be considered include linear multistep methods such as the leap frog and Adams-Bashforth schemes and one step multistage methods such as the classical Runge-Kutta schemes. The one-step multistage schemes have the advantages that they require no special start-up procedure, and they can readily be tailored to give a desired stability region. They have proved extremely effective in practice as a method of solving the Euler equations.

Let w^n be the result after n steps. The general form of an m-stage scheme is

$$\begin{aligned}
w^{(0)} &= w^n \\
w^{(1)} &= w^{(0)} - \alpha_1 \Delta t R^{(0)} \\
&\cdots \\
w^{(m-1)} &= w^{(0)} - \alpha_{m-1} \Delta t R^{(m-2)} \\
w^{(m)} &= w^{(0)} - \Delta t R^{(m-1)} \\
w^{n+1} &= w^{(m)}
\end{aligned} \tag{32}$$

The residual in the $(q+1)$th stage is evaluated as

$$R^{(q)} = \sum_{r=0}^{q} \beta_{qr} R(w^{(r)}) \tag{33}$$

where

$$\sum_{r=0}^{q} \beta_{qr} = 1$$

In the simplest case,

$$R^{(q)} = R(w^{(q)})$$

It is then known how to choose the coefficients α_q to maximize the stability interval along the imaginary axis and consequently the time step.[59] Since only the steady-state solution is needed, it pays to separate the residual $R(w)$ into its convective and dissipative parts $Q(w)$ and $D(w)$, respectively. The residual in the $(q+1)$th stage is now evaluated as

$$R^{(q)} = \sum_{r=0}^{q} \{\beta_{qr} Q(w^{(r)}) - \gamma_{qr} D(w^{(r)})\} \tag{34}$$

where

$$\sum_{r=0}^{q} \beta_{qr} = 1, \qquad \sum_{r=0}^{q} \gamma_{qr} = 1$$

Blended multistage schemes of this type, which have been analyzed in Ref. 60, can be tailored to give large stability intervals along both the imaginary and negative real axes.

The properties of multistage schemes can be further enhanced by residual averaging.[60] Here the residual at a mesh point is replaced by a weighted average of neighboring residuals. The average is calcualted implicitly. In a one-dimensional case $R(w)$ is replaced by $\bar{R}(w)$, where at the jth mesh point,

$$-\epsilon \bar{R}_{j-1} + (1+2\epsilon)\bar{R}_j - \epsilon \bar{R}_{j+1} = R_j$$

It can easily be shown that the scheme can be stabilized for an arbitrarily large time step by choosing a sufficiently large value for ϵ. In a nondissipative one-dimensional case one needs

$$\epsilon \geqslant \frac{1}{4}\left[\left(\frac{\Delta t}{\Delta t^*}\right)^2 - 1\right]$$

where Δt^* is the maximum stable time step of the basic scheme, and Δt is the actual time step. The method can be extended to three dimensions by

using smoothing in product form

$$(1-\epsilon_x\delta_x^2)(1-\epsilon_y\delta_y^2)(1-\epsilon_z\delta_z^2)\bar{R}=R \tag{35}$$

where δ_x^2, δ_y^2, and δ_z^2 are second difference operators in the coordinate directions, and ϵ_x, ϵ_y, and ϵ_z are the corresponding smoothing coefficients. Residual averaging can also be used on triangular meshes.[41] The implicit equations are then solved by a Jacobian iteration.

One can anticipate that implicit schemes will yield convergence in a smaller number of time steps, since the time step is no longer constrained by a stability limit. However, this will only pay if the decrease in the number of time steps outweighs the increase in the computational effort per time step consequent upon the need to solve coupled equations. The prototype implicit scheme can be formulated by estimating $\partial w/\partial t$ at $t+\mu\Delta t$ as a linear combination of $R(w^n)$ and $R(w^{n+1})$. The resulting equation

$$w^{n+1}=w^n-\Delta t\{(1-\mu)R(w^n)-\mu R(w^{n+1}) \tag{36}$$

can be linearized as

$$\left(I+\mu\Delta t\frac{\partial R}{\partial w}\right)\delta w+\Delta t R(w^n)=0 \tag{37}$$

Equation (37) reduces to the Newton iteration if one sets $\mu=1$ and lets $\Delta t\to\infty$. In a three-dimensional case with an $N\times N\times N$ mesh, its bandwidth is of order N^2. Direct inversion requires a number of operations proportional to the number of unknowns multiplied by the square of the bandwidth, that is, $\mathcal{O}(N^7)$. This is prohibitive and forces the recourse to either an approximate factorization method or an iterative solution method.

The main possibilities for approximate factorization are the alternating-direction method and the LU decomposition method. The alternating-direction method, which may be traced back to the work of Gourlay and Mitchell,[61] was given an elegant formulation for nonlinear problems by Beam and Warming.[12] In a two-dimensional case Eq. (37) is replaced by

$$(I+\mu\Delta tD_xA)(I+\mu\Delta tD_yB)\delta w+\Delta tR(w)=0 \tag{38}$$

where D_x and D_y are difference operators approximating $\partial/\partial x$ and $\partial/\partial y$, and A and B are the Jacobian matrices,

$$A=\frac{\partial f}{\partial w},\qquad B=\frac{\partial g}{\partial w}$$

This may be solved in two steps.

Step 1:

$$(I+\mu\Delta tD_xA)\delta w^*=-\Delta tR(w)$$

Step 2:

$$(I + \mu \Delta t D_y B)\delta w = \delta w^*$$

Each step requires block tridiagonal inversions and may be performed in $\mathcal{O}(N^2)$ operations on an $N \times N$ mesh. The algorithm is amenable to vectorization by simultaneous solution of the tridiagonal equations along parallel coordinate lines. The method has been refined to a high level of efficiency by Pulliam and Steger,[16] and Yee has extended it to incorporate a TVD scheme.[54] Its main disadvantage is that its extension to three dimensions is inherently unstable according a Von Neumann analysis.

The idea of the LU decomposition method[17] is to replace the operator in Eq. (20) by the product of lower and upper block triangular factors L and U,

$$LU\delta w + \Delta t R(w) = 0 \tag{39}$$

Two factors are used independently of the number of dimensions, and the inversion of each can be accomplished by inversion of its diagonal blocks. The method can be conveniently illustrated by considering a one-dimensional example. Let the Jacobian matrix $A = \partial f/\partial w$ be split as

$$A = A^+ + A^-$$

where the eigenvalues of A^+ and A^- are positive and negative, respectively. Then we can take

$$L \equiv I + \mu \Delta t D_x^- A^+, \qquad U \equiv I + \mu \Delta t D_x^+ A^- \tag{40}$$

where D_x^+ and D_x^- denote forward- and backward-difference operators, respectively, approximating $\partial/\partial x$. The reason for splitting A is to ensure the diagonal dominance of L and U independently of Δt. Otherwise, stable inversion of both factors will only be possible for a limited range of Δt. A crude choice is

$$A^{\pm} = \tfrac{1}{2}(A \pm \rho I)$$

where ρ is at least equal to the spectral radius of A. If flux splitting is used in the calculation of the residual, it is natural to use the corresponding splitting for L and U. An interesting variation is to combine an alternating-direction scheme with LU decomposition in the different coordinate directions.[62,63]

If one chooses to adopt the iterative solution technique, the principal alternatives are variants of the Gauss-Seidel and Jacobian methods. These may be applied to either the nonlinear equation [Eq. (36)] or the linearized equation [Eq. (37)]. A Jacobian method of solving Eq. (36) can be formulated by regarding it as an equation.

$$w - w^{(0)} + \mu \Delta t R(w) + (1 - \mu)\, \Delta t R(w^{(0)}) = 0$$

to be solved for w. Here $w^{(0)}$ is a fixed value obtained as the result of the previous time step. Such a procedure is a variant of the multistage time-stepping scheme described by Eqs. (32) and (33). It has the advantage of permitting simultaneous or overlapped calculation of the corrections at every mesh point and is readily amenable to parallel and vector processing.

A symmetric Gauss-Seidel scheme has been successfully employed in several recent works.[64] Consider the case of a flux split scheme in one dimension, for which

$$R(w) = D_x^+ f^-(w) + D_x^- f^+(w)$$

where the flux is split so that the Jacobian matrices

$$A^+ = \frac{\partial f^+}{\partial w} \qquad \text{and} \qquad A^- = \frac{\partial f^-}{\partial w}$$

have positive and negative eigenvalues, respectively. Now Eq. (37) becomes

$$\{I + \mu\Delta t(D_x^+ A^- + D_x^- A^+)\}\delta w + \Delta t R(w) = 0$$

At the jth mesh point this is

$$\{I + \alpha(A_j^+ - A_j^-)\}\delta w_j + \alpha A_{j+1}^- Dw_{j+1} - \alpha A_{j-1}^+ \delta w_{j-1} + \Delta t R_j = 0$$

where

$$\alpha = \mu \frac{\Delta t}{\Delta x}$$

Set $\delta w_j^{(0)} = 0$. A two-sweep-symmetric Gauss-Seidel scheme is then

Sweep 1:

$$\{I + \alpha(A_j^+ - A_j^-)\}\delta w_j^{(1)} - \alpha A_{j-1}^+ \delta w_{j-1}^{(1)} + \Delta t R_j = 0$$

Sweep 2:

$$\{I + \alpha(A_j^+ - A_j^-)\}\delta w_1^{(2)} + \alpha A_{j+1}^- \delta w_{j+1}^{(2)} - \alpha A_{j-1}^+ \delta w_{j-1}^{(1)} + \Delta t R_j = 0$$

Subtracting sweep 1 from sweep 2 we find that

$$\{I + \alpha(A_j^+ - A_j^-)\}\delta w_j^{(2)} + \alpha A_{j+1}^- \delta w_{j+1}^{(2)} = \{I + \alpha(A_j^+ - A_j^-)\}\delta w_j^{(1)}$$

Define the lower triangular, upper triangular, and diagonal operators L, U, and D as

$$L \equiv I - \alpha A^- + \mu\Delta t D_x^- A^+$$

$$U \equiv I + \alpha A^+ + \mu\Delta t D_x^+ A^-$$

$$D \equiv I + \alpha(A^+ - A^-)$$

It follows that the scheme can be written as

$$LD^{-1}U\delta w = -\Delta t R(w)$$

The iteration is usually terminated after one double sweep. The scheme is then a variation of an LU implicit scheme.

Some of these interconnections are illustrated in Fig. 6. Schemes in three main classes appear to be the most appealing:

1) variations of multistage time stepping, including the application of Jacobian iterative method to the implicit scheme (indicated by a single asterisk);

2) variations of LU decomposition, including the application of a Gauss-Seidel iterative method to the implicit scheme (indicated by a double asterisk); and

3) alternating-direction schemes, including schemes in which an LU decomposition is separately used in each coordinate direction (indicated by a triple asterisk).

The optimal choice may finally depend on the computer architecture. One might anticipate that the Guass-Seidel method of iteration could yield a faster rate of convergence than a Jacobian method, and it appears to be a particularly natural choice in conjunction with a flux split scheme that yields diagonal dominance. However, this class of schemes restricts the use of vector or parallel processing. Multistage time stepping, or Jacobian iteration of the implicit scheme allows maximal use of vector or parallel processing. The alternating-direction formulation removes any restriction on the time step (at least in the two-dimensional case), while permitting vectorization along coordinate lines. The *ADI-LU* scheme is an interesting compromise.

Acceleration Methods: Multigrid Technique

Clearly one can anticipate more rapid convergence to a steady state as the time step is increased. Accordingly, the rate of convergence of an explicit scheme can generally be substantially improved by using a variable time step close to the local stability limit throughout the flowfield. Assuming that the mesh cells are clustered near the body and expand as one moves away from the body, this effectively increases the rate at which disturbances are propagated through the outer part of the mesh. A similar strategy also pays with implicit schemes. In this case the terms in Δt^2 or Δt^3 resulting from factorization become dominant if Δt is too large, and the optimum rate of convergence is typically realized with a time step corresponding to a Courant number on the order of 10.

Further radical improvements in the convergence rate can be realized by the multigrid time-stepping technique, which extends the multigrid concept to the treatment of hyperbolic systems. Whereas relaxation methods for elliptic equations typically force the solution towards equilibrium by repeated smoothing, the transient behavior of hyperbolic systems is generally dominated by wave propagation. Accordingly, it seems that it should be possible to accelerate the evolution of the system to a steady state by using

large time steps on coarse grids, so that disturbances are more rapidly expelled through the outer boundaries. This is a quite different mechanism for convergence from smoothing. However, the interpolation of corrections back to the fine mesh will introduce errors that cannot be rapidly expelled from the fine mesh and should be locally damped if a fast rate of convergence is to be attained. Thus, it remains important that the driving scheme should have the property of rapidly damping out high-frequency modes. A relatively simple way to analyze the behavior of multigrid time-stepping schemes is proposed in Ref. 23.

A novel multigrid time-stepping scheme was proposed by Ni[21] in 1981. In his scheme the flow variables are stored at the mesh nodes, and the rates of change of mass, momentum, and energy in each mesh cell are estimated from the flux integral appearing in Eq. (20). The corresponding change δw_0 associated with the cell is then distributed unequally between the nodes at its four corners by the rule

$$\delta w_0 = \tfrac{1}{4}(\delta w_0 \pm A\delta w_0 \pm B\delta w_0)$$

where δw_0 is the correction at a corner, and A and B are the Jacobian matrices. The signs are varied in such a way that the accumulated corrections at each node correspond to the first two terms of a Taylor series in time, like a Lax-Wendroff scheme. When several grid levels are used, the distribution rule is applied once on each level down to the coarsest grid, and the corrections are then interpolated back to the fine grid. Distributed correction schemes of this type have been further developed by Hall,[65] with very good results. They have also been extended to the Navier-Stokes equations by Chima and Johnson.[66]

An alternative formulation of multigrid time-stepping schemes was proposed by the present author.[22] This formulation, which can be combined with a variety of time-stepping schemes, corresponds to the full approximation scheme of Brandt.[20] It is most easily described by using subscripts to indicate the grid level. Several transfer operations need to be defined. First, the solution vector on grid k must be initialized as

$$w_k^{(0)} = T_{k,k-1} w_{k-1}$$

where w_{k-1} is the current value on grid $k-1$, and $T_{k,k-1}$ is a transfer operator. Next, it is necessary to transfer a residual forcing function such that the solution on grid k is driven by the residuals calculated on grid $k-1$. This can be accomplished by setting

$$P_k = Q_{k,k-1} R_{k-1}(w_{k-1}) - R_k(w_k^{(0)})$$

where $Q_{k,k-1}$ is another transfer operator. Then $R_k(w_k)$ is replaced by $R_k(w_k) + P_k$ in the time-stepping scheme. For example, the multistage

scheme defined by Eq. (32) is reformulated as

$$w_k^{(1)} = w_k^{(0)} - \alpha_1 \Delta t_k (R_k^{(0)} + P_k)$$

$$\cdots$$

$$w_k^{(q+1)} = w_k^{(0)} - \alpha_{q+1} \Delta t_k (R_k^{(q)} + P_k)$$

$$\cdots$$

The result $w_k^{(m)}$ then provides the initial data for grid $k+1$. Finally, the accumulated correction on grid k has to be transferred back to grid $k-1$. Let w_k^+ be the final value of w_k resulting from both the correction calculated in the time step on grid k and the correction transferred from grid $k+1$. Then one sets

$$w_{k-1}^+ = w_{k-1} + I_{k-1,k}(w_k^+ - w_k^{(0)})$$

where w_{k-1} is the solution on grid $k-1$ after the time step on grid $k-1$ and before the transfer to grid k, and $I_{k-1,k}$ is an interpolation operator. A W cycle of the type illustrated in Fig. 7 proves to be a particularly effective strategy for managing the work split between the meshes.

Both cell-centered and vertex-based schemes can be devised along these lines,[22,23,67] and they seem to work about equally well. With properly optimized coefficients the multistage time-stepping scheme is a very efficient driver of the multigrid process. Some results are presented in Figs. 8 and 9. Figure 8 shows a result for the RAE 2822 airfoil computed on an O mesh with 160 cells around the profile and 32 cells in the normal direction. This was obtained with a five-stage time-stepping scheme in which the dissipative terms were evaluated three times in each step. A cell-centered formulation was used for the space discretization, with adaptive dissipation of the type defined by Eqs. (29) and (30). The average residual measured by the rate of change of the density was reduced from 0.124 to 0.219×10^{-10} in 100-W cycles. This corresponds to an average reduction of 0.797 per cycle. The solution after 10 cycles is also displayed, and it can be seen that the solution is virtually identical. The lift coefficient is 1.1258 after 10 cycles and 1.1256 after 100 cycles. Figure 9 shows a three-dimensional calculation for a swept wing using a vertex scheme on a $192 \times 32 \times 48$ mesh. In this case the mean convergence rate over 100 cycles is 0.8222, and a fully converged result is obtained in 25 cycles. Computer times for these calculations are small enough their use in an that interactive design method could be contemplated. A two-dimensional calculation with 10 cycles on a 160×32 mesh can be performed on a Cray in several seconds. A three-dimensional calculation with 15 cycles on a $96 \times 16 \times 16$ mesh requires about 25 s using one processor of a Cray XMP.

Alternating-direction and LU implicit time-stepping schemes, as well as symmetric relaxation schemes, have been explored as alternatives to the multistage time-stepping procedure as a driver of the multigrid scheme.[68-71]

They are also effective. Very good results have been obtained by Anderson et al.,[72] who used an *ADI* scheme with Van Leer flux splitting, and by Hemker and Spekreijse,[73] who used relaxation with Osher flux splitting. Multigrid methods have also been extended to unstructured triangular meshes.[74,75]

Grid Generation and Complex Geometry

If computational methods are to be really useful to airplane designers, they must be able to treat extremely complex configurations, ultimately extending up to a complete aircraft. A major pacing item in the effort to attain this goal has been the problem of mesh generation. For simple wing-body combinations it is possible to generate rectilinear meshes without too much difficulty.[76] For more complicated configurations containing, for example, pylon-mounted engines, it becomes increasingly difficult to produce a structured mesh that is aligned with the body surface.

A wide variety of grid-generation techniques have been explored by numerous investigators. Algebraic transformations can be used to generate grids for quite complex shapes.[77,78] A popular alternative, pioneered by Thompson et al.,[79] is to generate grid surfaces as solutions of elliptic equations. Hyperbolic marching methods have also proved successful in some applications.[80]

The algebraic and elliptic methods can be extended to treat more complex configurations by dividing the flowfield into subdomains and generating the mesh in separate blocks. The mesh blocks may be required to match at the interfaces,[81] or they may be allowed to overlap each other.[82] A striking example of what can be achieved by these methods is exhibited in the work of Sawada and Takanashi,[83] who have calculated the flow over a four-engined short takeoff aircraft with overwing nacelles, using a flux-difference-split upwind discretization of the Euler equations.

An alternative procedure is to use tetrahedral cells in an unstructured mesh that can be adapted to conform to the complex surface of an aircraft. References 84 and 85 present a method based on such an approach. Separate overlapping meshes are generated around the individual components to create a cluster of points surrounding the whole aircraft. The swarm of mesh points is then connected together to form tetrahedral cells that provide the basis for a single finite-element approximation for the entire domain. This use of triangulation to unify separately generated meshes bypasses the need to devise interpolation procedures for transferring information between overlapping meshes. The triangulation of a set of points is in general nonunique. The method adopted in this work is to generate the Delaunay triangulation,[86] which is dual to the Voronoi diagram[87] that results from a division of the domain into polyhedral neighborhoods, each consisting of the subdomain of points nearer to a given mesh point than to any other mesh point. The Euler equations are discretized by establishing conservation of mass, momentum, and energy in polyhedral control volumes with a three-dimensional generalization of Eq. (25) and are solved by a multistage time-stepping scheme.

Figures 10a–10c and Plates 1–3 (see the color section) illustrate a transonic flow solution about a McDonnell Douglas MD-11 commercial transport aircraft at cruise conditions. The surface grid and flow solution are displayed with closeup views that emphasize the details of the engine regions. In the solution figures, high-pressure regions and low-pressure areas are shaded black, whereas near-freestream areas are very light. In the plates blue indicates regions of low velocity, and red indicates regions of high velocity. Flow is allowed through the nacelles and core-cowls (which are modeled as open tubes) without specification of mass flux. Discretization of the flowfield is accomplished with an unstructured mesh that contains 334,595 nodes and 1,953,286 packed tetrahedrons. The aircraft's surface is described with 34,521 triangles. A solution of this type currently requires about .4 Cray 2 CPU hours for the grid generation and nearly 4 Cray 2 CPU hours for a 300-iteration flow solution that reduces the residuals 3.5 orders of magnitude. Both the grid generation and flow solution use 50 megawords of core for this case.

Viscous Flow Calculations

Boundary-Layer Corrections

Although it is true that the viscous effects are relatively unimportant outside the boundary layer, the presence of the boundary layer can have a drastic influence on the pattern of the global flow. This will be the case, for example, in the event that the flow separates. The boundary layer can also cause global changes in a lifting flow by changing the circulation. These effects are particularly pronounced in transonic flows. The presence of a boundary layer can cause the location of the shock wave on the upper surface of the wing to shift 20% of the chord.

Although we must generally account for the presence of the boundary layer, the accuracy attainable in solutions of the Navier-Stokes equations for complete flowfields is severely limited by the extreme disparity between the length scales of the viscous effects and those of the gross patterns of the global flow. This has encouraged the use of methods in which the equations of viscous flow are solved only in the boundary layer, and the external flow is treated as inviscid. These zonal methods can give very accurate results in many cases of practical concern to the aircraft designer. The underlying ideas have been comprehensively reviewed in papers by Lock and Firmin,[88] Le Balleur,[89] and Melnik.[90]

In the outer region the real viscous flow is approximated by an equivalent inviscid flow, which has to be matched to the inner viscous flow by an appropriate selection of boundary conditions. In most of the boundary layer the viscous flow equations may consistently be approximated by the boundary-layer equations. This is sufficient in regions of weak interaction, in which the viscous effect on the pressure is small. However, there are regions of strong interaction in which the classical boundary-layer formulation fails, because of the appearance of strong normal pressure gradients across the boundary layer. Coupling conditions for the interaction between the inner viscous flow and the outer inviscid flow can be derived from an

asymptotic analysis in which the Reynolds number is assumed to become very large. The coupled viscous and inviscid equations are solved iteratively. Semi-inverse methods in which transpiration boundary conditions are prescribed for both the inviscid flow calculation and the boundary-layer analysis have allowed these methods to be extended to treat flows with separated regions.[91,92]

The method of Bauer et al.[93] was the first to incorporate boundary-layer corrections into the calculation of transonic potential flow. This method only accounted for displacement effects on the airfoil and modeled the wake as a parallel semi-infinite strip. Nevertheless, this simple model substantially improved the agreement with experimental data. Several more complete theoretical models, including effects due to the wake thickness and curvature, have been developed.[94–96]

The simulation of attached flows by zonal methods now rests on a firm theoretical foundation and has reached a high level of sophistication in practice. The treatment of three-dimensional flows is presently limited by a lack of available boundary-layer codes for general configurations. Zonal methods have the disadvantage that extensions to more general configurations require a separate asymptotic analysis of each component region, such as the corner between a wing and a nacelle pylon, with the result that they can become unmanageable as the complexity of the configuration is increased.

Reynolds-Averaged Navier-Stokes Equations

Advances in algorithms and also in the speed and memory of currently available computers have brought us to a point where solutions of the Reynolds-averaged Navier-Stokes equations are entirely feasible for both two- and three-dimensional flows. The hope is that it will be possible to develop a fairly universal method that will be able to predict separated flows where present zonal methods fail. The principal requirements for a satisfactory solution of the Reynolds-averaged Navier-Stokes equations include the following:

1) the reductions of the discretization errors to a level such that any numerically introduced dissipative terms are much smaller than the real viscous terms; and

2) the closure of the equations by a turbulence model that accurately represents the turbulent stresses.

The development of the necessary numerical methods is already quite advanced. The methods described in the previous section can generally be carried over to the Navier-Stokes equations. The viscous terms can be discretized by standard techniques for numerical approximation.

The principal difficulty in producing an adequate numerical approximation is the need to use a mesh with very fine spacing in the direction normal to the wall to resolve the extreme gradients in the boundary layer. Typically it has been found that there should be of the order of 32 intervals inside the boundary layer and another 32 intervals between the boundary layer and the far field. Meshes of this type generally contain cells with a very high aspect ratio, on the order of 1000, adjacent to the wall and in the wake

region. When the aspect ratio of the cells becomes so large, discretization schemes are prone to suffer both loss of accuracy and attrition of their rate of convergence to a steady state. These difficulties can be remedied by very careful control of the numerical dissipation introduced by the discretization and improvements in the iterative scheme.

The recent Viscous Transonic Airfoil Workshop at the 25th AIAA Aerospace Sciences Meeting provided an opportunity to assess the current state of the art. Results were presented for a variety of different numerical methods and turbulence models. Among the more highly developed methods were those of Coakley,[97] who used an upwind flux-split scheme with a variety of turbulence models, Rumsey et al.,[98] who used an upwind scheme with Van Leer splitting and a Baldwin-Lomax turbulence model, and Maksymiuk and Pulliam,[99] who used the ARC2D program with central differencing and a Baldwin-Lomax turbulence model. All three of these methods use alternating-direction time-stepping schemes. King showed the results of substituting alternative turbulence models in ARC2D, including the recently developed Johnson and King model.[100] Results obtained by the rational Runge-Kutta method with a Baldwin-Lomax turbulence model were presented by Morinishi and Satofuka.[101] A comparison of these results indicates that simulations using quite different numerical methods were in excellent agreement with each other as long as they used the same turbulence model, but that a change in the turbulence model could produce a drastic change in the solution, particularly in the case of a strong shock-induced separation. Predictions using the Baldwin-Lomax model agree quite well with experimental data when the flow is attached or only slightly separated, but an examination of the velocity profile in the boundary layer indicates that the model does not correctly represent the shock-wave–boundary-layer interaction. The two-equation models tested by Coakley showed no substantial improvement. The new Johnson and King model produced a better simulation of strongly separated flows, but seemed to be less accurate in the regions of attached flow.

An extension of the multigrid multistage scheme to treat the Navier-Stokes equations was presented in Ref. 103. This method is the subject of ongoing research to improve its accuracy and efficiency,[104] and some recently obtained results are presented in Figs. 11–14. The first two figures show a verification of the ability of the method to produce accurate Euler solutions on meshes with very-high-aspect-ratio cells, designed to resolve the boundary layer in Navier-Stokes calculations. Figure 11 shows a shock-free Euler solution for the Korn airfoil[93] on a 320×64 Navier-Stokes mesh, obtained in 50 multigrid cycles. Figure 12 shows an Euler solution for the RAE 2822 airfoil on a 512×64 Navier-Stokes mesh. This is case 9 from Ref. 102, and the experimental data are also displayed. Figure 13 shows the prediction obtained for the same case using the Baldwin-Lomax turbulence model. This result also agrees well with the result obtained by Coakley for this case using the Baldwin-Lomax model. Figure 14 shows the same calculation with the lower-order artificial dissipation defined by $\epsilon^{(2)}$ in Eq. (38) deleted. It can be seen that essentially the same result is obtained. Apparently the high-order dissipative terms are sufficient for numerical stability, and the shock wave is captured without

oscillations with the aid of the eddy viscosity. These calculations exhibit a less rapid rate of convergence to a steady state than Euler calculations on less highly bunched meshes. Nevertheless, 100–200 cycles have consistently proved sufficient for convergence in numerous calculations.

Usefully accurate three-dimensional Navier-Stokes simulations are now also within the range of existing supercomputers. This has been demonstrated by the calculations of Shang and Scherr[105] and Fujii and Obayashi.[106] Chandler and MacCormack[107] have recently developed an effective relaxation method for the Navier-Stokes equations.

Conclusion

Computational aerodynamics has come of age during the last two decades, and in several of its branches it is now a mature discipline. Some of the more striking successes, which have been referred to in this necessarily incomplete survey point the way to its future acceptance as a primary tool for aerodynamic analysis and design. Basic numerical algorithms for the treatment of viscous and compressible flows with shock waves are now in hand, and rapidly convergent solution methods are well established. The concepts of total variation diminishing difference schemes and multigrid acceleration methods, in particular, provide examples that mathematical elegance can be just as important in the development of computational methods as it has been for analytical methods.

Some areas of likely concentration for future research can be identified. These include the following

1) The quest for numerical approximation schemes with a higher order of accuracy: The power of the spectral method[108,109] for numerical approximation of smooth solutions beckons efforts to extend it to treat discontinuous solutions. It is already used as an effective tool in simulations of turbulence.[110] The recently proposed concept of essentially nonoscillatory (ENO) schemes[111] is another interesting direction of research.

2) Front tracking: Ultimately, it should be possible to attain improved representation of shock waves and contact discontinuities by treating them as internal boundaries.[112] The use of triangular meshes offers new opportunities to represent more complex features such as triple points.

3) Adaptive mesh redistribution and refinement: It is clear that greatly improved accuracy can be attained for a given computational cost by adapting the mesh to the solution as it develops during the calculation. This can be a key to obtaining adequate resolutions of all the important features of really complex flows, and it may be an effective alternative to front tracking for the representation of discontinuities. Widespread research on the realization of adaptive methods is in progress.[113–117] Repeated local subdivision ultimately destroys any coherence of the structure of the mesh, and unstructured triangular meshes provide a natural basis for the use of such a procedure.[74,75,116,117]

4) Concurrent computation: The best opportunity for further increases in computing speed lies in the use of concurrent computation, which may be realized through the introduction of vector, pipelined, and parallel

arithmetic processors. Algorithms of the future must be designed to take full advantage of these architectures.

5) Optimization and design: An aerodynamic analysis may warn a designer that his proposed configuration is unsatisfactory, but it is not very helpful to him if it provides no indication of how to make an improvement. Ultimately, computational methods for aerodynamic analysis ought to be incorporated in automatic design procedures, which will use computer optimization methods, and perhaps expert systems to refine and improve the configuration. Some early efforts have already demonstrated the feasibility of automatic design.[118,119]

6) Turbulence modeling: Improved simulations of separated viscous flows will require advances in turbulence modeling. More complex multiequation formulations may be necessary for the realization of more universally applicable models. Renormalization group theory offers another avenue towards the construction of a rational turbulence model.[120]

Once these various challenges have been surmounted, the simulation of both external and internal flows will become a routine practice. Methods of the future must be capable of treating arbitrary configurations, including complex aircraft, and flows in complex propulsive systems. Simulations for hypersonic aircraft will require the inclusion of real gas effects and chemical reactions at high temperatures. New ideas will surely be brought to bear on some of these problems.

References

[1]Jones, R. T., "Properties of Low Aspect Ratio Pointed Wings at Speeds Below and Above the Speed of Sound," NACA Rept. TR-835, 1946.

[2]Hayes, W. D., "Linearized Supersonic Flow," North American Aviation Rept. AL-222, 1947.

[3]Whitcomb, R. T., "A Study of the Zero Lift Drag-Rise Characteristics of Wing-Body Combinations Near the Speed of Sound," NACA TR-1273, 1956.

[4]Whitcomb, R. T., "Reviews of NASA Supercritical Airfoils," ICAS Paper 74-10, 1974.

[5]Hess, J. L., and Smith, A. M. O., "Calculation of Non-Lifting Potential Flow About Arbitrary Three-Dimensional Bodies," Douglas Aircraft Rept. ES 40622, 1962.

[6]Rubbert, P. E., and Saaris, G. R., "A General Three-Dimensional Potential Flow Method Applied to V/STOL Aerodynamics," Society of Automotive Engineers Paper 680304, 1968.

[7]Woodward, F. A., "An Improved Method for the Aerodynamic Analysis of Wing-Body-Tail Configurations in Subsonic and Supersonic Flow, Part 1—Theory and Application," NASA CR-2228, May 1973.

[8]Murman, E. M., and Cole, J. D., "Calculation of Plane Steady Transonic Flows," *AIAA Journal*, Vol. 9, No. 1, 1971, pp. 114–121.

[9]Murman, E. M., "Analysis of Embedded Shock Waves Calculated by Relaxation Methods," *AIAA Journal*, Vol. 12, No. 5, 1974, pp. 626–633.

[10]Magnus, R., and Yoshihara, H., "Inviscid Transonic Flow Over Airfoils," *AIAA Journal*, Vol. 8, No. 12, 1970, pp. 2157–2162.

[11]MacCormack, R. W., "The Effect of Viscosity in Hyper-Velocity Impact Cratering," AIAA Paper 69-354, 1969.

[12]Beam, R. W., and Warming, R. F., "An Implicit Finite Difference Algorithm for Hyperbolic System in Conservation Form," *Journal of Computational Physics*, Vol. 23, 1976, pp. 87–110.

[13]Steger, J. L., "Implicit Finite Difference Simulation of Flow About Arbitrary Two Dimensional Geometries," *Journal of Computational Physics*, Vol. 16, 1978, pp. 679–686.

[14]Steger, J. L., and Warming, R. F., "Flux Vector Splitting of the Inviscid Gas Dynamics Equations with Applications to Finite Difference Methods," *Journal of Computational Physics*, Vol. 40, 1981, pp. 263–293.

[15]Rizzi, A., and Viviand, H., "Numerical Methods for the Computation of Inviscid Transonic Flows with Shock Waves," *Proceedings of the GAMM Workshop*, Vieweg, 1981.

[16]Pulliam, T. H., and Steger, J. L., "Implicit Finite Difference Simulations of Three-Dimensional Compressible Flow," *AIAA Journal*, Vol. 18, No. 2, 1980, pp. 159–167.

[17]Jameson, A., and Turkel, E., "Implicit Schemes and LU Decompositions," *Math. Comp.*, Vol. 37, 1981, pp. 385–397.

[18]Jameson, A., Schmidt, W., and Turkel, E., "Numerical Solution of the Euler Equations by Finite Volume Methods Using Runge-Kutta Time Stepping Schemes," AIAA Paper 81-1259, 1981.

[19]Fedorenko, R. P., "The Speed of Convergence of One Iterative Process," *USSR Computational Mathematics and Mathematical Physics*, Vol. 4, 1964, pp. 227–235.

[20]Brandt, A., "Multi-Level Adaptive Solutions to Boundary Value Problems," *Math. Comp.*, Vol. 31, 1977, pp. 333–390.

[21]Ni, R. H., "A Multiple Grid Scheme for Solving the Euler Equations,' *AIAA Journal*, Vol. 20, No. 11, 1982, pp. 1565–1571.

[22]Jameson, A., "Solution of the Euler Equations by a Multigrid Method," *Applied Math. and Computation*, Vol. 13, 1983, pp. 327–356.

[23]Jameson, A., "Multigrid Algorithms for Compressible Flow Calculations," *Lecture Notes in Mathematics*, Vol. 1228, edited by W. Hackbusch and V. Trottenberg, Springer-Verlag, 1986, pp. 166–201.

[24]Chapman, D. R., "Computational Aerodynamics Development and Outlook," *AIAA Journal*, Vol. 17, No. 12, 1979, pp. 1293–1313.

[25]Jameson, Antony, "Iterative Solution of Transonic Flows Over Airfoils and Wings, Including Flows at Mach 1," *Comm. Pure. Appl. Math.*, Vol. 27, 1974, pp. 283–309.

[26]Albone, C. M., "A Finite Difference Scheme for Computing Supercritical Flows in Arbitrary Coordinate Systems," Royal Aircraft Establishment Rept. 74090, 1974.

[27]Jameson, A., "Transonic Potential Flow Calculations in Conservation Form," *Proceedings of AIAA 2nd Computational Fluid Dynamics Conference*, AIAA, New York, 1975, pp. 148–161.

[28]Eberle, A., "A Finite Volume Method for Calculating Transonic Potential Flow Around Wings from the Minimum Pressure Integral," NASA TM-75324, translated from MBB UFE 1407(0), 1978.

[29]Hafez, M., South, J. C., and Murman, E. M., "Artificial Compressibility Method for Numerical Solutions of Transonic Full Potential Equation," *AIAA Journal*, Vol. 17, No. 8, 1979, pp. 838–844.

[30]Holst, T. L., and Ballhaus, W. F., "Fast Conservative Schemes for the Full Potential Equation Applied to Transonic Flows," *AIAA Journal*, Vol. 17, No. 2, 1979, pp. 145–152.

[31]Ballhaus, W. F., Jameson, A., and Albert, J., "Implicit Approximate Factorization Schemes for Steady Transonic Flow Problems," *AIAA Journal*, Vol. 16, No. 6, 1978, pp. 573–579.

[32]Holst, T. L., and Thomas, S. D., "Numerical Solution of Transonic Wing Flow Fields," AIAA Paper 82-0105, 1982.

[33]South, J. C., and Brandt, A., "Application of a Multi-Level Grid Method to Transonic Flow Calculations," *Proceedings of Workshop on Transonic Flow Problems in Turbomachinery, Monterey, 1976*, edited by T. C. Adamson and M. F. Platzer, Hemisphere, Washington, DC, 1977, pp. 180–206.

[34]Hackbusch, W., "On the Multi-Grid Method Applied to Difference Equations," *Computing*, Vol. 20, 1978, pp. 291–306.

[35]Jameson, A., "Acceleration of Transonic Potential Flow Calculations on Arbitrary Meshes by the Multiple Grid Method," *Proceedings of AIAA 4th Computational Fluid Dynamics Conference*, AIAA, New York, 1979, pp. 122–146.

[36]Jameson, A., and Caughey, D. A., "A Finite Volume Method for Transonic Potential Flow Calculations," *Proceedings of AIAA 3rd Computational Fluid Dynamics Conference*, AIAA, New York, 1977, pp. 35–54.

[37]Bristeau, M. O., Glowinski, R., Periaux, J., Perrier, P., Pirronneau, O., and Poirier, G., "On the Numerical Solution of Nonlinear Problems in Fluid Dynamics by Least Squares and Finite Element Methods (II), Application to Transonic Flow Simulations," *Computer Methods in Applied Mechanics and Engineering*, Vol. 51, 1985, pp. 363–394.

[38]Giles, M., Drela, M., and Thompkins, W. T., "Newton Solution of Direct and Inverse Transonic Euler Equations," AIAA Paper 85-1530, 1985.

[39]Lax, P. D., and Wendroff, B., "Systems of Conservation Laws," *Comm. Pure Appl. Math.*, Vol. 13, 1960, pp. 217–237.

[40]MacCormack, R. W., and Paullay, A. J., "Computational Efficiency Achieved by Time Splitting of Finite Difference Operators," AIAA Paper 72-154, 1972.

[41]Jameson, A., and Mavriplis, D., "Finite Volume Solution of the Two-Dimensional Euler Equations on a Regular Triangular Mesh," AIAA Paper 85-0435, Jan. 1985.

[42]Jameson, A., "Current Status of Future Directions of Computational Transonics," *Computational Mechanics—Advances and Trends*, edited by A. K. Noor, American Society of Mechanical Engineers, New York, Publ. AMD 75, 1986.

[43]Gudonov, S. K., "A Difference Method for the Numerical Calculation of Discontinuous Solutions of Hydrodynamic Equations," *Mathematicheskii Sbornik*, Vol. 47, 1959, pp. 271–306; translated as JPRS 7225 by U.S. Dept. of Commerce, 1960.

[44]Boris, J. P., and Book, D. L., "Flux Corrected Transport, I SHASTA, A Fluid Transport Algorithm that Works," *Journal of Computational Physics*, Vol. 11, 1973, pp. 38–69.

[45]Van Leer, B., "Towards the Ultimate Conservative Difference Scheme. II Monotonicity and Conservation Combined in a Second Order Scheme," *Journal of Computational Physics*, Vol. 14, 1974, pp. 361–370.

[46]Van Leer, B., "Flux Vector Splitting for the Euler Equations," *Proceedings of the 8th International Conference on Numerical Methods in Fluid Dynamics, Aachen, 1982*, edited by E. Krause, Springer-Verlag, Berlin, 1982, pp. 507–512.

[47]Roe, P. L., "Approximate Riemann Solvers, Parameter Vectors, and Difference Schemes," *Journal of Computational Physcs*, Vol. 43, 1981, pp. 357–372.

[48]Osher, S., and Solomon, F., "Upwind Difference Schemes for Hyperbolic Systems of Conservation Laws," *Math. Comp.*, Vol. 38, 1982, pp. 339–374.

[49]Harten, A., "High Resolution Schemes for Hyperbolic Conservation Laws," *Journal of Computational Physics*, Vol. 49, 1983, pp. 357–393.

[50]Osher, S., and Chakravarthy, S., "High Resolution Schemes and the Entropy Condition," *Journal of Numerical Analysis*, Vol. 21, 1984, pp. 955–984.

[51]Sweby, P. K., "High Resolution Schemes Using Flux Limiters for Hyperbolic Conservation Laws," *SIAM Journal of Numerical Analysis*, Vol. 21, 1984, pp. 995–1011.

[52]Anderson, B. K., Thomas, J. L., and Van Leer, B., "A Comparison of Flux Vector Splittings for the Euler Equations," AIAA Paper 85-0122, Jan. 1985.

[53]Jameson, A., "Nonoscillatory Shock Capturing Scheme Using Flux Limited Dissipation," *Large Scale Computations in Fluid Mechanics*, Vol. 22, Pt. 1, edited by B. E. Engquist, S. Osher, and R. C. J. Sommerville, American Mathematical Society, Providence, RI, 1985, pp. 345–370 (Lectures in Applied Mathematics).

[54]Yee, H. C., "On Symmetric and Upwind TVD Schemes," *Proceedings of the 6th GAMM Conference on Numerical Methods in Fluid Mechanics, Göttingen*, FRG, *Sept. 1985.*

[55]Lax, P. D., "Hyperbolic Systems of Conservation Laws and the Mathematical Theory of Shock Waves," *SIAM Regional Series on Applied Mathematics*, Vol. 11, 1973.

[56]Jameson, A., and Lax, P. D., "Conditions for the Construction of Multi-point Total Variation Diminishing Schemes," *Applied Numerical Mathematics*, Vol. 2, 1986, pp. 335–345.

[57]Goodman, J. B., and Leveque, R. J., "On the Accuracy of Stable Schemes for 2-D Scalar Conservation Laws," *Math. Comp.*, Vol. 45, 1985, pp. 15–21.

[58]Yoon, S., and Jameson, A., "An LU Implicit Scheme for High Speed Inlet Analysis," AIAA Paper 86-1520, June 1986.

[59]Kinmark, I. P. E., "One Step Integration Methods with Large Stability Limits for Hyperbolic Partial Differential Equations," *Advances in Computer Methods for Partial Differential Equations*, Vol. V, edited by R. Vichnevetsky and R. S. Stepleman, IMACS, 1984, pp. 345–349.

[60]Jameson, A., "Transonic Flow Calculations for Aircraft," *Numerical Methods in Fluid Dynamics*, Vol. 1127, edited by F. Brezzi, Springer-Verlag, Berlin, 1985, pp. 156–242 (Lecture Notes in Mathematics).

[61]Gourlay, A. R., and Mitchell, A. R., "A Stable Implicit Difference Method for Hyperbolic Systems in Two Space Variables," *Numer. Math.*, Vol. 8, 1966, pp. 367–375.

[62]Obayashi, S., and Kuwakara, K., "LU Factorization of an Implicit Scheme for the Compressible Navier Stokes Equations," AIAA Paper 84-1670, June 1984.

[63]Obayashi, S., Matsukima, K., Fujii, K., and Kuwakara, K., "Improvements in Efficiency and Reliability for Navier-Stokes Computations Using the LU-ADI Factorization Algorithm," AIAA Paper 86-0338, Jan. 1986.

[64]Chakravarthy, S. R., "Relaxation Methods for Unfactored Implicit Upwind Schemes," AIAA Paper 84-0165, Jan. 1984.

[65]Hall, M. G., "Cell Vertex Multigrid Schemes for Solution of the Euler Equations," IMA Conference on Numerical Methods for Fluid Dynamics, Reading, MA, April 1985.

[66]Chima, R. V., and Johnson, G. M., "Efficient Solution of the Euler and Navier Stokes Equations with a Vectorized Multiple-Grid Algorithm," AIAA Paper 83-1893, 1983.

[67]Jameson, A., "A Vertex Based Multigrid Algorithm for Three Dimensional Compressible Flow Calculations," *Numerical Methods for Compressible Flow—Finite Difference, Element and Volume Techniques*, edited by T. E. Tezduar and T. J. R. Hughes, Americal Society of Mechanical Engineers, New York, Publ. AMD 78, 1986.

[68]Jameson, A., and Yoon, S., "Multigrid Solution of the Euler Equations Using Implicit Schemes," AIAA Paper 85-0293, Jan. 1985.

[69]Jameson, A., and Yoon, S., "LU Implicit Schemes with Multiple Grids for the Euler Equations," AIAA Paper 86-0105, Jan. 1986.

[70]Yoon, S., Choo, Y. K., and Jameson, A., "An LU-SSOR Scheme for the Euler and Navier Stokes Equations," AIAA Paper 87-0599, Jan. 1987.

[71]Caughey, D. A., "A Diagonal Implicit Multigrid Algorithm for the Euler Equations," AIAA Paper 87-453, Jan. 1987.

[72]Anderson, W. K., Thomas, J. L., and Whitfield, D. L., "Multigrid Acceleration of the Flux Split Euler Equations," AIAA Paper 86-0274, Jan. 1986.

[73]Hemker, P. W., and Spekreijse, S. P., "Multigrid Solution of the Steady Euler Equations," Proc. Oberwolfach Meeting on Multigrid Methods, FRG, Dec. 1984.

[74]Jameson, A., and Mavriplis, D., "Multigrid Solution of the Euler Equations on Unstructured and Adaptive Meshes," Third Copper Mountain Conference on Multigrid Methods, Copper Mountain, April 1985.

[75]Lallemand, M. H., and Dervieux, A., "A Multigrid Finite Element Method for Solving the Two Dimensional Euler Equations," Third Copper Mountain Conference on Multigrid Methods, Copper Mountain, April 1988.

[76]Baker, T. J., "Mesh Generation by a Sequence of Transformations," *Applied Numerical Mathematics*, Vol. 2, 1986, pp. 515–528.

[77]Eiseman, P. R., "A Multi-Surface Method of Coordinate Generation," *Journal of Computational Physics*, Vol. 33, 1979, pp. 118–150.

[78]Eriksson, L. E., "Generation of Boundary-Conforming Grids around Wing-Body Configurations using Transfinite Interpolation," *AIAA Journal*, Vol. 20, No. 10, 1982, pp. 1313–1320.

[79]Thomspon, J. F., Thames, F. C., and Mastin, C. W., "Automatic Numerical Generation of Body-Fitted Curvilinear Coordinate System for Field Containing any Number of Arbitrary Two-Dimensional Bodies," *Journal of Computational Physics*, Vol. 15, 1974, pp. 299–319.

[80]Steger, J. L., and Chaussee, D. S., "Generation of Body-Fitted Coordinates Using Hyperbolic Partial Differential Equations," *SIAM Journal of Scientific and Statistical Computing*, Vol. 1, 1980, pp. 431–437.

[81]Weatherill, N. P., and Forsey, C. R., "Grid Generation and Flow Calculations for Aircraft Geometries," *Journal of Aircraft*, Vol. 22, No. 10, 1985, pp. 855–860.

[82]Benek, J. A., Buning, P. G., and Steger, J. L., "A 3-D Chimera Grid Embedding Technique," AIAA Paper 85-1523, June 1985.

[83]Sawada, K., and Takanashi, S., "A Numerical Investigation on Wing/Nacelle Interferences of USB Configurations," AIAA Paper 87-0455, Jan. 1987.

[84]Jameson, A., Baker, T. J., and Weatherhill, N. P., "Calculation of Inviscid Transonic Flow over a Complete Aircraft," AIAA Paper 86-0103, Jan. 1986.

[85]Jameson, A., and Baker, T. J., "Improvements to the Aircraft Euler Method," AIAA Paper 87-0452, Jan. 1987.

[86]Delaunay, B., "Sur la Sphere Vide," *Bulletin of the Academy of Sciences of the USSR VII: Class Scil. Mat. Nat.*, 1934, pp. 793–800.

[87]Voronoi, G., "Nouvelles Applications des Parametres Continus a la Theorie des Formes Quadratiques. Deuxieme Memoire: Recherches Sur les Parallell oedres Primitifs," *Journal Reine Angew. Math.*, Vol. 134, 1908, pp. 198–287.

[88]Lock, R. C., and Firmin, M. C. P., "Survey of Techniques for Estimating Viscous Effects in External Aerodynamics," *Proceedings of the IMA Conference on Numerical Methods in Aeronautical Fluid Dynamics, Reading, 1980*, edited by P. L. Roe, Academic, New York, 1982, pp. 337–430.

[89]Le Balleur, J. C., "Numerical Viscid-Inviscid Interaction in Steady and Unsteady Flows," Proceedings of the 2nd Symposium on Numerical and Physical Aspects of Aerodynamic Flows, Long Beach, CA, 1983.

[90]Melnik, R. E., "Turbulent Interactions on Airfoils at Transonic Speeds—Recent Developments," AGARD CP-291, Paper 10, 1980.

[91]Carter, J. E., "A New Boundary Layer Inviscid Iteration Technique for Separated Flow," *Proceedings of AIAA 4th Computational Fluid Dynamics Conference*, AIAA, New York, 1979, pp. 45–55.

[92]Le Balleur, J. C., "Strong Matching Methods of Computing Transonic Viscous Flow Including Wakes and Separations—Lifting Airfoils, "*La Recherche Aerospátiále*, Vol. 3, 1981.

[93]Bauer, F., Garabedian, P., Korn, D., and Jameson, A., *Supercritical Wing Sections*, Vol. II, Springer-Verlag, New York, 1975.

[94]Le Balleur, J. C., Peyret, R., and Viviand, H., "Numerical Studies in High Reynolds Number Aerodynamics," *Computers and Fluids*, Vol. 8, 1980, pp. 1–30.

[95]Collyer, M. R., and Lock, R. C., "Prediction of Viscous Effects in Steady Transonic Flow Past an Aerofoil," *Aeronautical Quarterly*, Vol. 30, 1979, pp. 485–505.

[96]Melnik, R. E., Chow, R. R., Mead, H. R., and Jameson, A., "A Multigrid Method for the Computation of Viscid/Inviscid Interaction on Airfoils," AIAA Paper 83-0234, 1983.

[97]Coakley, T. J., "Numerical Simulation of Viscous Transonic Airfoil Flows," AIAA Paper 87-0416, Jan. 1987.

[98]Rumsey, C. L., Taylor, S. L., Thomas, J. L., and Anderson, W. K., "Application of an Upwind Navier-Stokes Code to Two-Dimensional Transonic Airfoil Flow," AIAA Paper 87-0413, Jan. 1987.

[99]Maksymiuk, C. M., and Pulliam, T. H., "Viscous Transonic Airfoil Workshop Results Using ARC2D," AIAA Paper 87-0415, Jan. 1987.

[100]King, L. S., "A Comparison of Turbulence Closure Models for Transonic Flows About Airfoils," AIAA Paper 87-0418, Jan. 1987.

[101]Morinishi, K., and Satofuka, N., "A Numerical Study of Viscous Transonic Flows Using RRK Scheme," AIAA Paper 87-0426, Jan. 1987.

[102]Cook, P. H., McDonald, M. A., and Firmin, M. C. P., "Aerofoil RAE 2822 Pressure Distributions, and Boundary Layer and Wake Measurements," AGARD Advisory Rept. 138, 1979.

[103]Martinelli, L., Jameson, A., and Grasso, F., "A Multigrid Method for the Navier Stokes Equations," AIAA Paper 86-0208, Jan. 1986.

[104]Martinelli, L., "Calculations of Viscous Flows with a Multigrid Method," MS Thesis, Princeton Univ., Princeton, NJ, May 1987.

[105]Shang, J. S., and Scherr, S. J., "Navier Stokes Solution of the Flow Field Around a Complete Aircraft," AIAA Paper 85-1509, July 1985.

[106]Fujii, K., and Obayashi, S., "Navier Stokes Simulation of Transonic Flow Over Wing-Fuselage Combinations," AIAA Paper 86-1831, June 1986.

[107]Chandler, G. V., and MacCormack, R. W., "Hypersonic Flow Past 3-D Configurations," AIAA Paper 87-0480, Jan. 1987.

[108]Orszag, S., and Gottlieb, D., "Numerical Analysis of Spectral Methods," *SIAM Regional Series on Applied Mathematics*, Vol. 26, 1977.

[109]Canuto, C., Hussaini, M. Y., Quarteroni, A., and Zang, D. A., "Spectral Methods in Fluid Dynamics" (to be published).

[110]Hussaini, M. Y., "Stability, Transition and Turbulence," Proceedings of the NASA Symposium on Supercomputing in Aerospace, NASA CP-2454, March 1987.

[111]Chakravarthy, S. R., Harten, A., and Osher, S., "Essentially Non-Oscillatory Shock Capturing Schemes of Uniformly Very High Accuracy," AIAA Paper 86-0339, Jan. 1986.

[112]Moretti, G., "An Efficient Euler Solver, with Many Applications," AIAA Paper 87-0352, Jan. 1987.

[113]Dwyer, H. A., Smooke, M. O., and Kee, R. J., "Adaptive Grid Method for Problems in Fluid Mechanics and Heat Transfer," *AIAA Journal*, Vol. 18, No. 10, 1980, pp. 1205–1212.

[114]Berger, M., and Jameson, A., "Automatic Adaptive Grid Refinement for the Euler Equations," *AIAA Journal*, Vol. 23, No. 4, 1985, pp. 561–568.

[115]Dannenhoffer, J. F., and Baron, J. R., "Robust Grid Adaptation for Complex Transonic Flows," AIAA Paper 86-0495, Jan. 1986.

[116]Lohner, R., Morgan, K., and Peraire, J., "Improved Adaptive Refinement Strategies for the Finite Element Aerodynamic Configurations," AIAA Paper 86-0499, Jan. 1986.

[117]Holmes, D. G., and Lamson, S. H., "Adaptive Triangular Meshes for Compressible Flow Solutions," *Proceedings of the International Conference on Numerical Grid Generation in Computational Fluid Dynamics, Landshut, July 1986*, edited by J. Hauser and C. Taylor, Pineridge, Swansea, UK, 1986, pp. 413–424.

[118]Hicks, R. M., and Henne, P. A., "Wing Design by Numerical Optimization," AIAA Paper 79-0080, 1979.

[119]Gregg, R. D., and Misegades, K., "Transonic Wing Optimization Using Evolution Theory," AIAA Paper 87-0520, Jan. 1987.

[120]Yakhot, V., and Orszag, S., "Renormalization Group Analysis of Turbulence. 1. Basic Theory," *Journal of Scientific Computing*, Vol. 1, 1986, pp. 3–51.

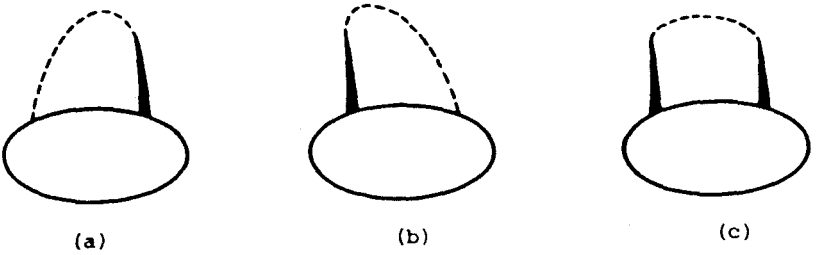

Fig. 1 Alternative solutions for an ellipse: a) compression shock; b) expansion shock; c) symmetric shock.

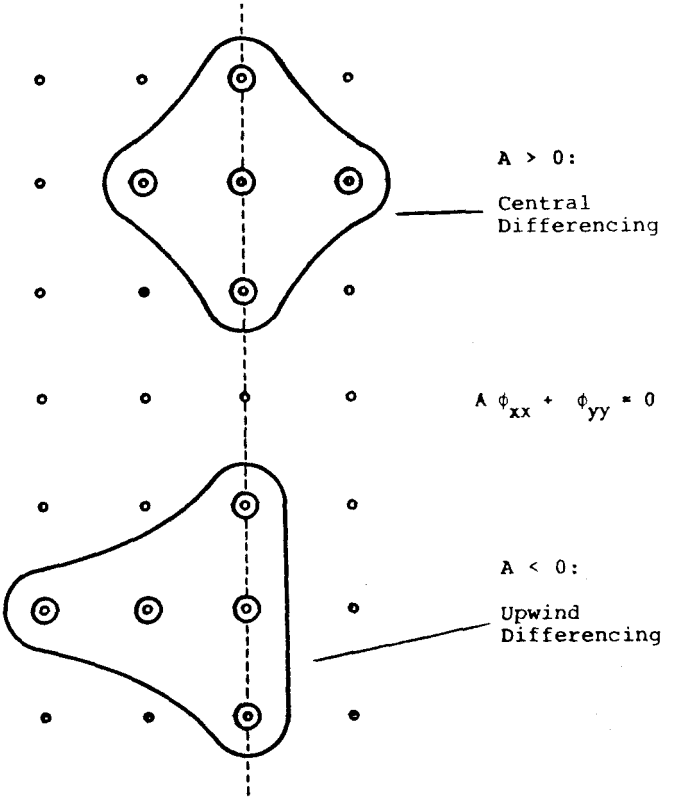

Fig. 2 Murman-Cole difference scheme.

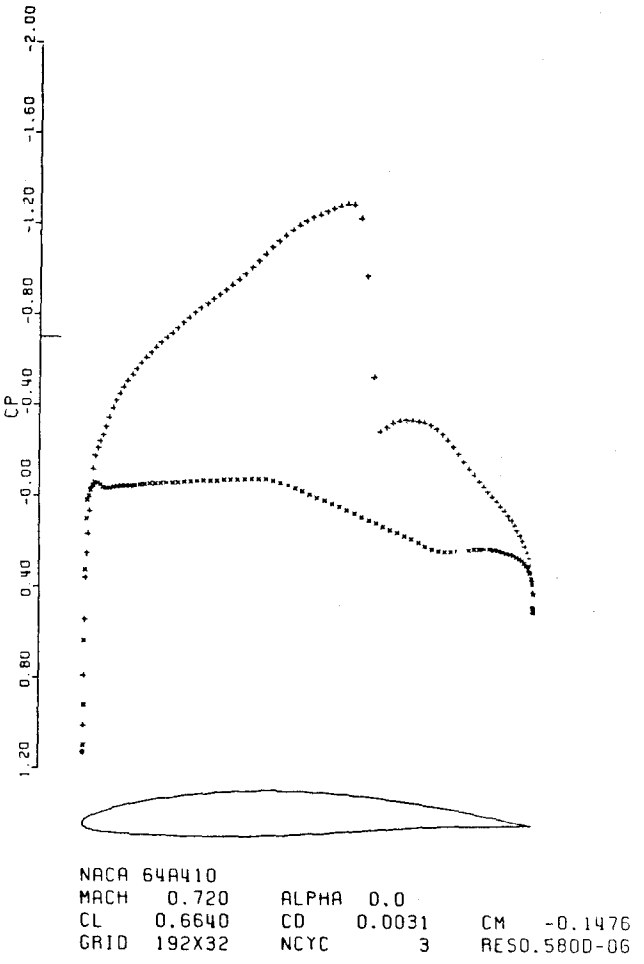

Fig. 3 Transonic potential-flow solution calculated with three multigrid V cycles.

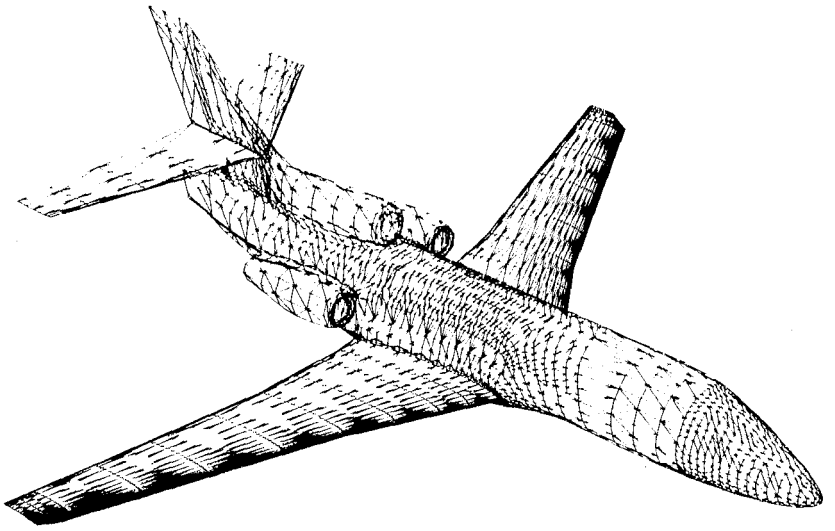

Fig. 4a Surface mesh for transonic potential flow over a Falcon 50.

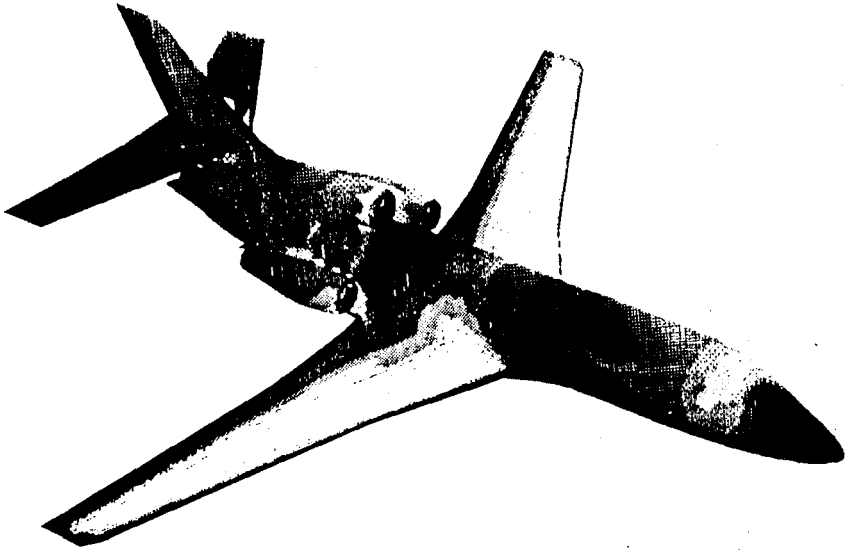

Fig. 4b Surface Mach contours for transonic potential flow over a Falcon 50.

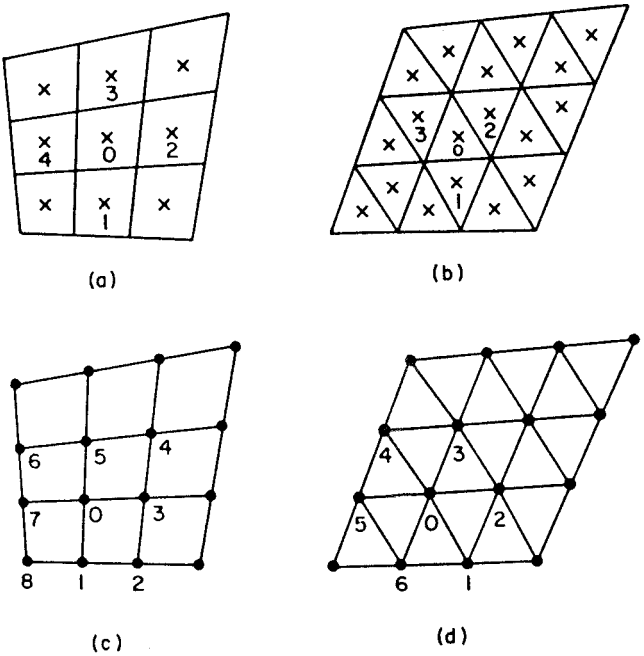

Fig. 5 Alternative discretization schemes: a) cell-centered rectilinear; b) cell-centered triangular; c) vertex rectilinear; d) vertex triangular.

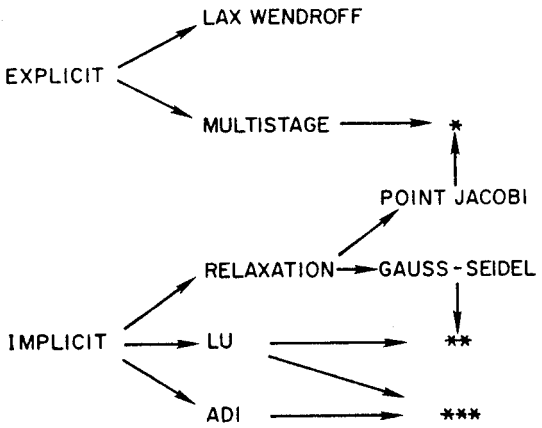

Fig. 6 Time-stepping schemes.

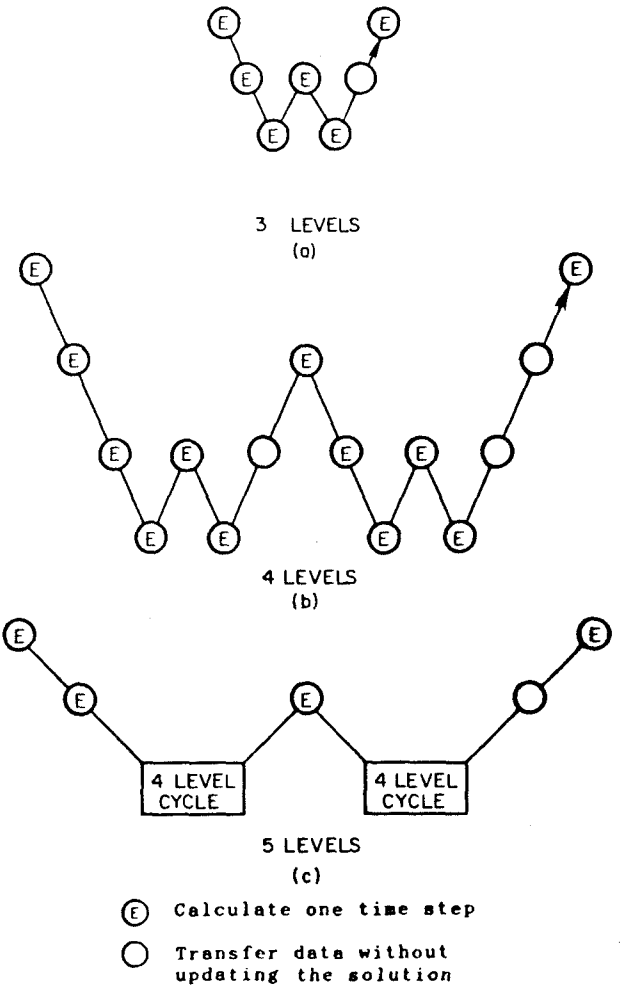
3 LEVELS
(a)
4 LEVELS
(b)
4 LEVEL CYCLE
4 LEVEL CYCLE
5 LEVELS
(c)
Calculate one time step
Transfer data without updating the solution

Fig. 7 *W* **cycle.**

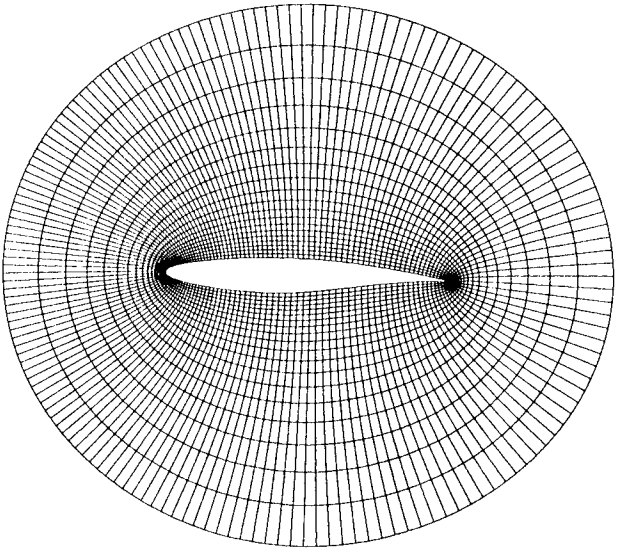

Fig. 8a Inner grid for Euler solution on RAE 2822 airfoil.

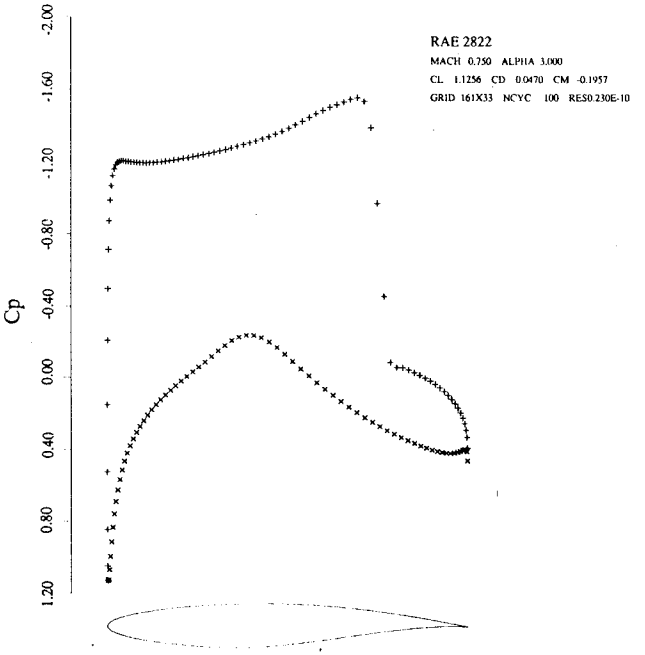

Fig. 8b Euler solution on RAE 2822 airfoil after 100 cycles.

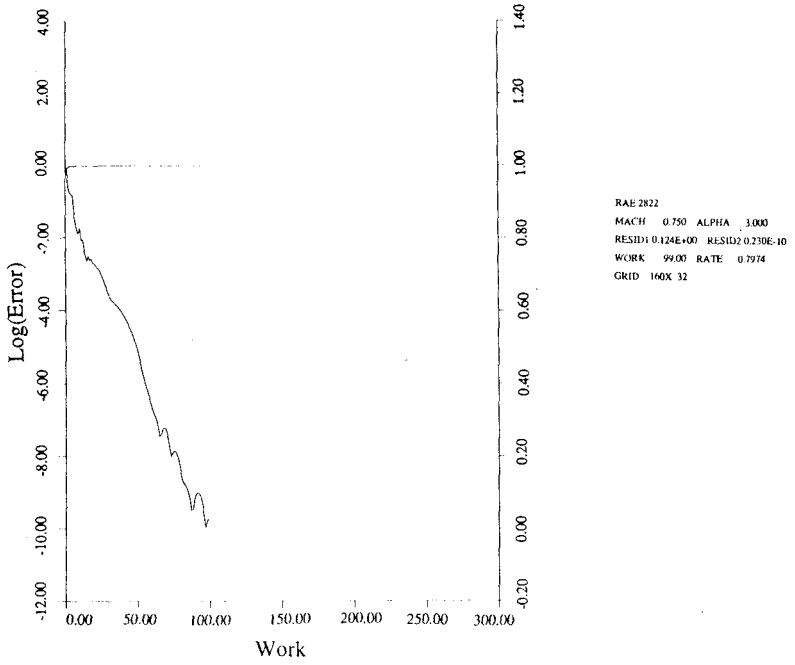

Fig. 8c Convergence history for Euler solution on RAE 2822 airfoil.

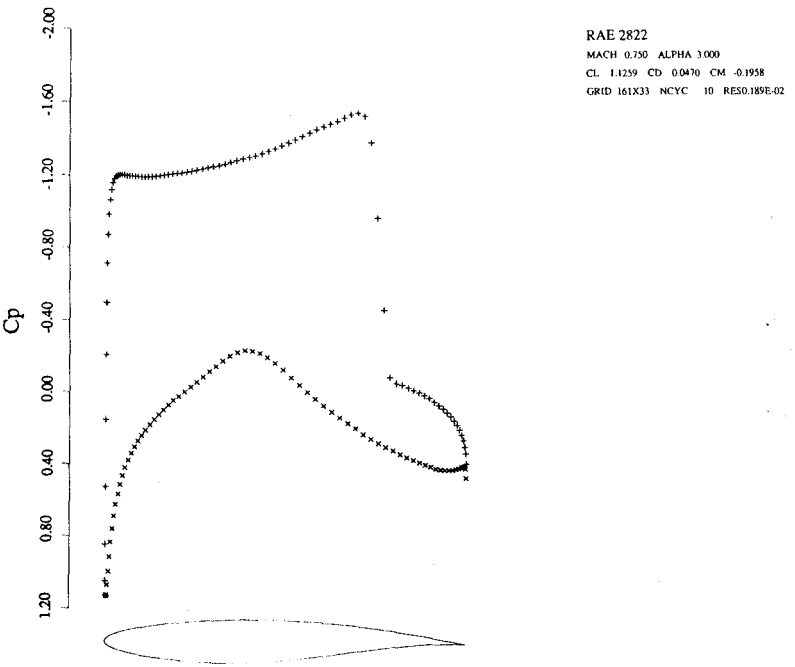

Fig. 8d Euler solution on RAE 2822 airfoil after 10 cycles.

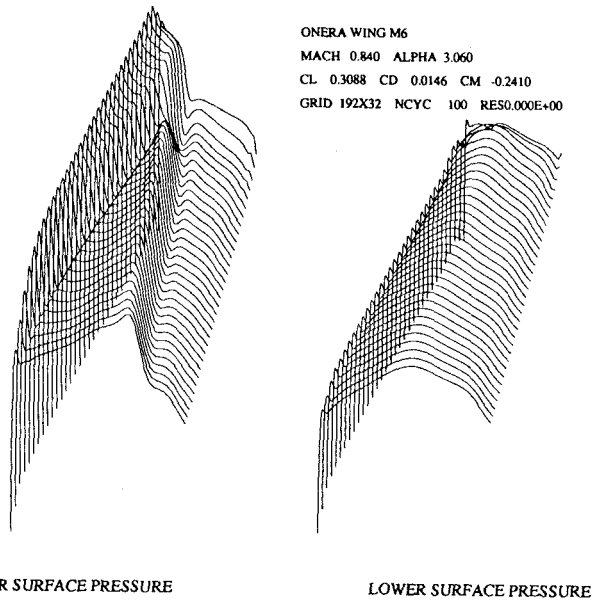

Fig. 9a Euler solution on ONERA M6 wing after 100 cycles.

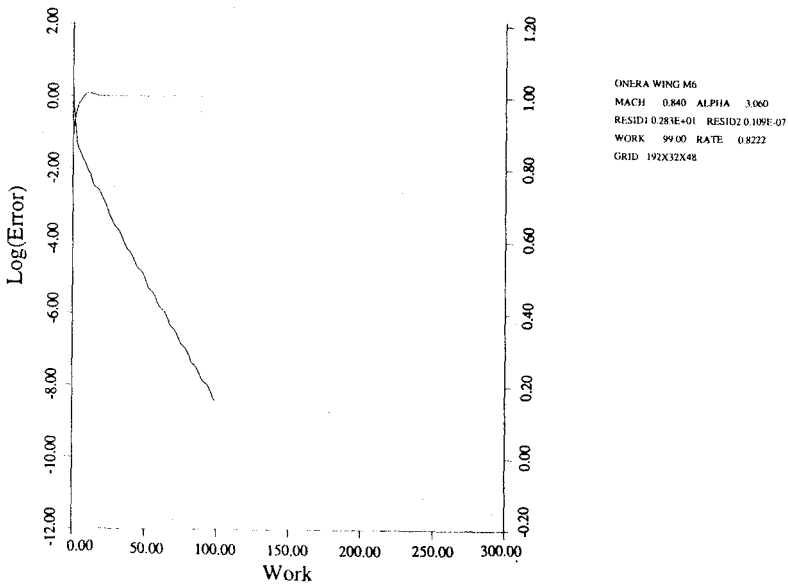

Fig. 9b Convergence history for Euler solution on ONERA M6 wing.

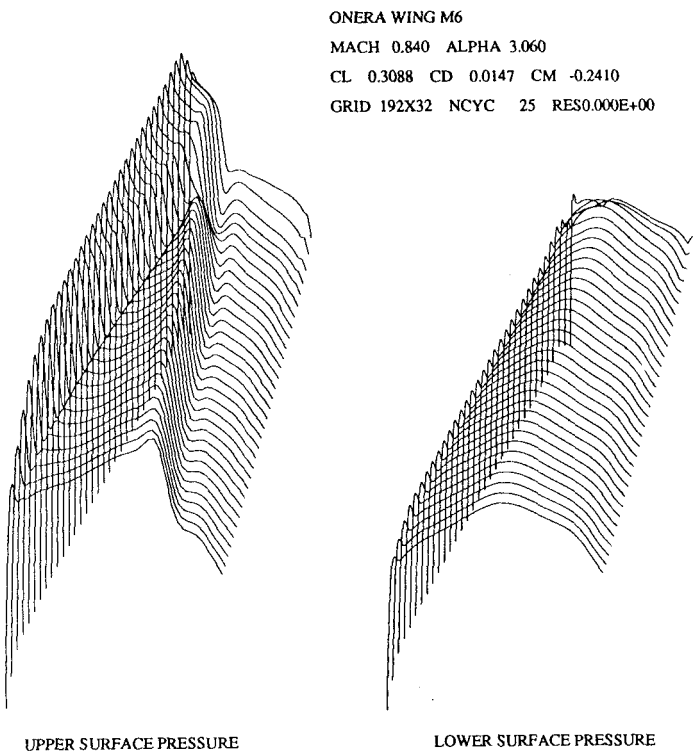

Fig. 9c Euler solution on ONERA M6 wing after 25 cycles.

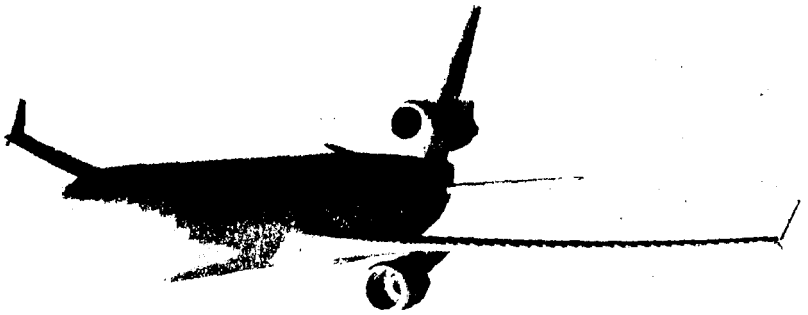

Fig. 10a McDonnell Douglas MD-11 transport shaded surfaces.

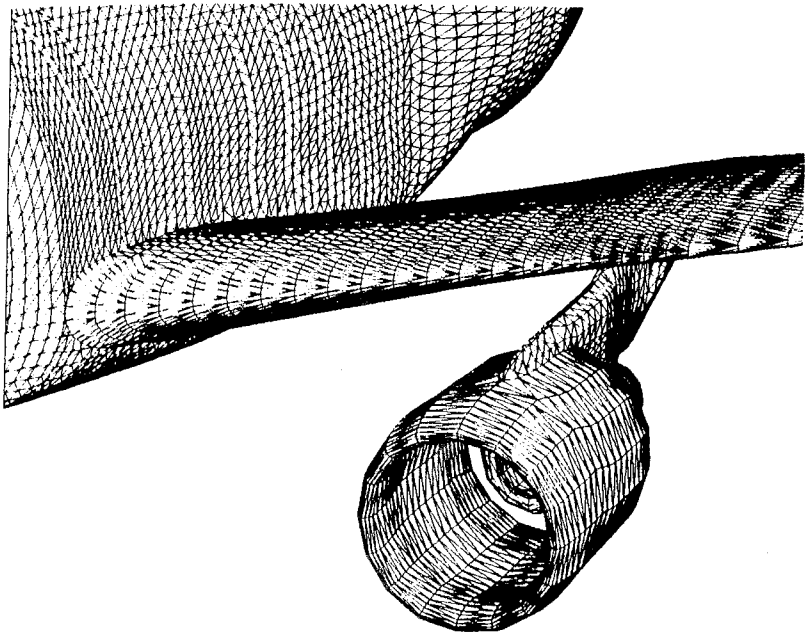

Fig. 10b Detailed grid for McDonnell Douglas MD-11 transport fuselage/wing pylon nacelle.

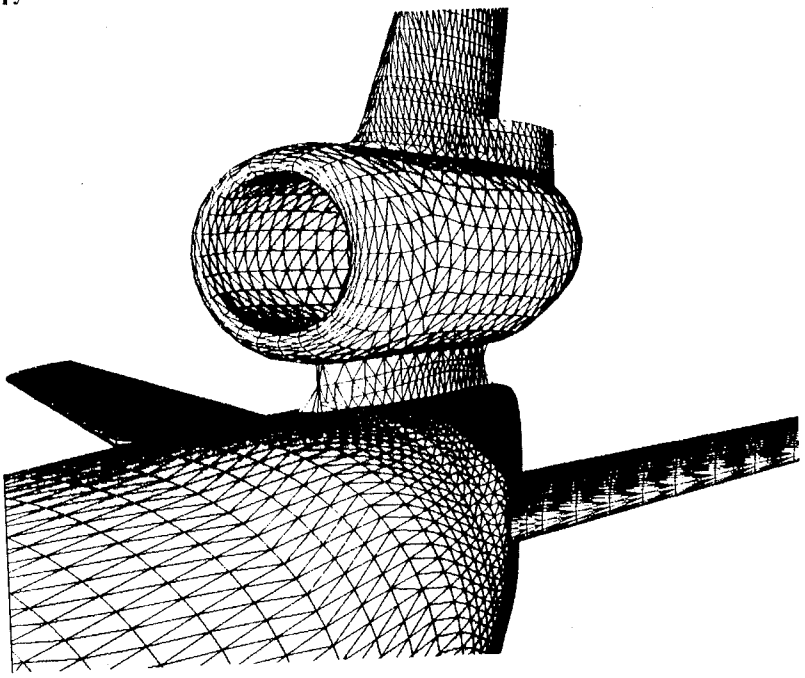

Fig. 10c Detailed grid for McDonnell Douglas MD-11 transport empennage/aft nacelle.

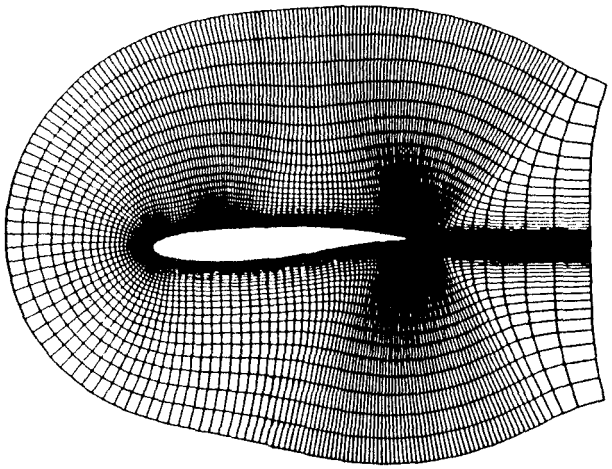

Fig. 11a Navier-Stokes mesh for Euler solution on Korn Airfoil.

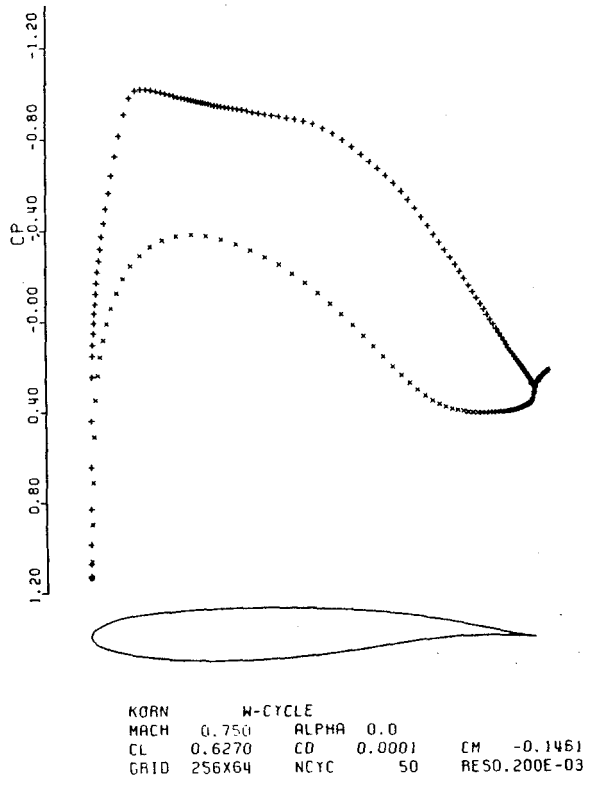

Fig. 11b Euler solution for Korn airfoil on Navier-Stokes mesh.

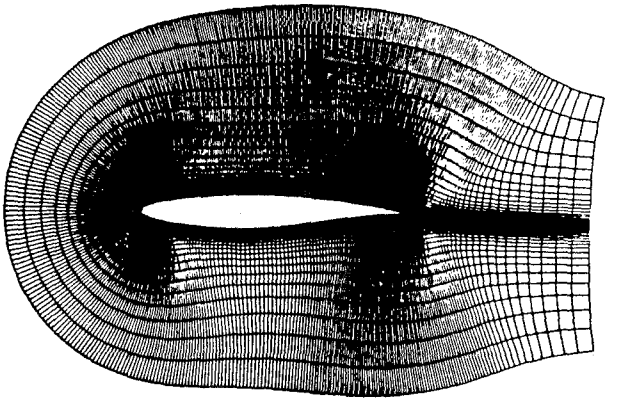

Fig. 12a 512 × 64 Navier-Stokes mesh for Euler solution on RAE 2822.

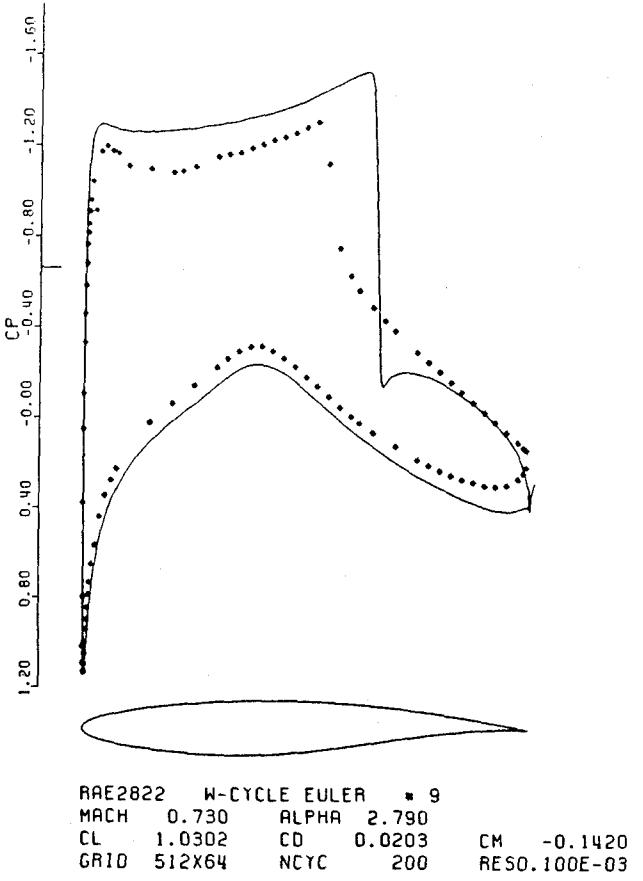

Fig. 12b Euler solution for RAE 2822 on Navier-Stokes mesh.

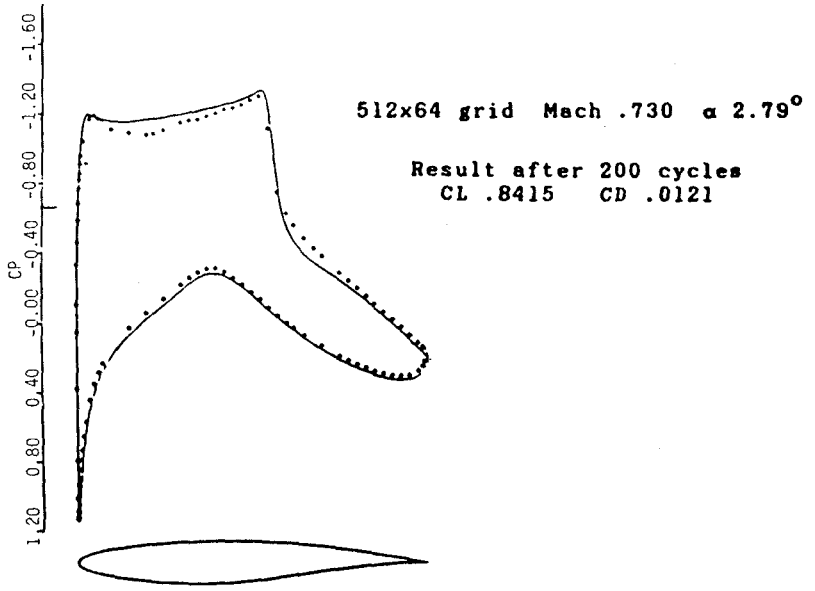

Fig. 13 Navier-Stokes solution for RAE 2822-Baldwin-Lomax turbulence model.

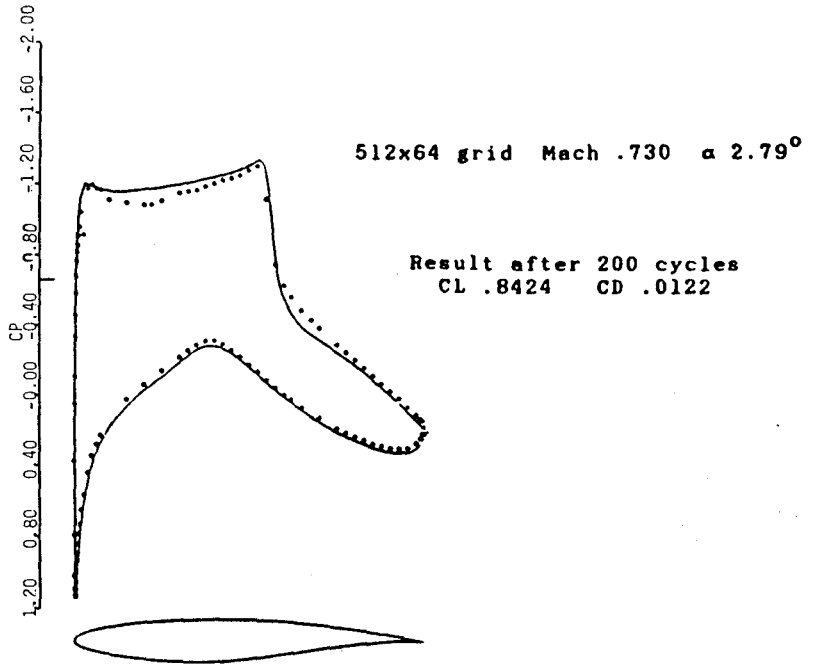

Fig. 14 Navier-Stokes solution for RAE 2822-Baldwin-Lomax turbulence model, artificial dssipation from fourth difference only.